JOURNAL OF PHYSIOLOGY AND PHARMACOLOGY 2018, 69, 3, 373-390
www.jpp.krakow.pl | DOI: 10.26402/jpp.2018.3.04

E. GOROWSKA-WOJTOWICZ[1], P. DUTKA[1], M. KUDRYCKA[1], P. PAWLICKI[1], A. MILON[1], B.J. PLACHNO[2], W. TWORZYDLO[3], L. PARDYAK[1], A. KAMINSKA[1], A. HEJMEJ[1], B. BILINSKA[1], M. KOTULA-BALAK[1]

REGULATION OF STEROIDOGENIC FUNCTION OF MOUSE LEYDIG CELLS: G-COUPLED MEMBRANE ESTROGEN RECEPTOR AND PEROXISOME PROLIFERATOR-ACTIVATED RECEPTOR PARTNERSHIP

[1]Department of Endocrinology, Institute of Zoology and Biomedical Research, Jagiellonian University in Cracow, Cracow, Poland;
[2]Department of Plant Cytology and Embryology; Institute of Botany, Jagiellonian University in Cracow, Cracow, Poland;
[3]Developmental Biology and Invertebrate Morphology; Institute of Zoology and Biomedical Research, Jagiellonian University in Cracow, Cracow, Poland

We tested whether G-coupled membrane estrogen receptor (GPER) and peroxisome proliferator activated receptor (PPAR) partnership exists and whether this interaction regulates mouse Leydig cell function. Mature and aged mice were treated with the antagonist of GPER (G-15; 50 μg/kg b.w). Leydig cells (MA-10) were treated with G-15 (10 nM) alone or in combination with peroxisome proliferator-activated receptor α or γ antagonists, respectively (PPARα, 10 μM; PPARγ, 10 μM). GPER blockage affected testis steroidogenic status *via* changes in lutropin and cholesterol levels as well as protein expression alterations of the lutropin receptor, acute steroidogenesis activating protein, translocator protein, and protein kinase A in mouse Leydig cells both *in vivo* and *in vitro*. Inactivation of both GPER and PPAR *in vitro* revealed expressional modulation of other steroidogenesis-controlling molecules acting on various steps of lipid homeostasis *e.g.* cytochrome P450scc, perilipin, hormone sensitive lipase, and 3-hydroxy-3-methyl-glutaryl-coenzyme A reductase. Concomitantly, microscopic analysis of cells treated with antagonists showed changes in morphology, migration competences and cytoskeleton structure. In the above processes, the action of GPER and PPARα was regulated through the PI3K/Akt pathway, while PPARγ was mediated by the Ras/Raf pathway. In addition, GPER and PPARs specifically controlled individual signaling proteins. For the first time, we report here the importance of GPER-PPARα and -PPARγ 'neopartnership' in maintenance of Leydig cell morpho-functional status.

Key words: *G-coupled estrogen receptor, Leydig cell, lutropin, perilipin, peroxisome proliferator-activated receptor, steroidogenesis*

INTRODUCTION

Leydig cells are interstitial cells located adjacent to the seminiferous tubules in the testes. These cells produce the sex steroid hormone, testosterone, under the pulsatile control of pituitary luteinizing hormone (LH). Steroidogenesis consists of initial cholesterol mobilization from lipid droplets and/or the plasma membrane and/or *de novo* synthesis (by the rate-limiting enzymes 3-hydroxy-3-methylglutaryl coenzyme A (HMG-CoA) synthase 1 (HMGCS1) and reductase (HMGCR)). Cholesterol is then transported into the mitochondria, converted to pregnenolone, which is subsequently converted into the final steroid products by enzymes of the smooth endoplasmic reticulum (1). LH plays two essential roles in Leydig cell steroidogenesis: it maintains optimal levels of steroidogenic enzymes (trophic regulation) and mobilizes and transports cholesterol into the inner mitochondrial membrane (acute regulation) with the involvement of intermediate molecules (*e.g.* cAMP-dependent kinase, PKA; acute steroidogenic regulatory protein, StAR; translocator protein, TSPO). Steroid biosynthesis is finely regulated by the phosphorylation-dephosphorylation of intermediate molecules, as well as number of signaling molecules involving receptor proteins (2). Thereby, many cellular responses, including steroid hormone action, require coordinated cross-talk between phosphorylating protein kinases and phosphatase activity.

The use of chemical agents that perturb the polymerization of cytoskeletal proteins has shed light on a key role for microfilaments and microtubules in the uptake and transport of cholesterol in steroidogenic cells. Sewer and Li (3) reported that mitochondria trafficking is dependent on microtubules, resulting in steroid hormone production at the step of cholesterol delivery to mitochondria. Thus, in steroidogenic cell activity, proper cytoskeletal function guarantees effective sex steroid production.

Peroxisome proliferator-activated receptors (PPARs) are nuclear receptors that are closely related to thyroid hormone or retinoid receptors. To date, three subtypes of PPARs have been described in amphibians, rodents, and humans: PPARα, PPARβ (also known as PPAR-δ), and PPARγ (4). PPARs target genes encoding enzymes involved in peroxisome and mitochondria function as well as action of the fatty acids, apolipoproteins, and lipoprotein lipase. Therefore, role of PPARs in lipid metabolism

and homeostasis is unchallenged. These receptors are highly expressed in liver, heart, intestine, and renal proximal tubules but their pathophysiological roles in these organs are only partially elucidated (5-7). Little is known about PPARs in the male reproductive system. In rat testis, PPARs are mainly expressed in Leydig and Sertoli cells but not in spermatogonial cells (8). It was shown that some PPAR chemicals alter testosterone production (9), and their long-term administration results in Leydig cell tumor development in rats (10).

PPAR can signal itself by ligand binding *e.g.* low-affinity ligands such as unsaturated long-chain fatty acids derived from nutrient uptake and/or inflammatory reactions (11). Of note, some synthetic drugs (*e.g.* thiazolidinediones) that modulate PPAR activity were approved as insulin sensitizers for the treatment of type-2 diabetes mellitus (12). Mechanisms of PPAR-ERK signaling crosstalk are well-described in cells with high energy metabolism as well as in tissue disorders (*e.g.* neurologic) (13). Such action includes (i) simultaneous activation of the ERK cascade (*e.g.*, by mitogens) therein contributing to inhibition of genomic action through serine phosphorylation of PPAR; (ii) activation of the ERK cascade by phosphorylation of transcription factors that interact with PPAR; (iii) nuclear export and cytoplasmic retention of PPAR by MEK1 resulting in 'off-DNA'-interaction of PPAR with distinct protein partners (*e.g.*, cytoskeleton, lipid droplets, kinases) leading to alternative cytoplasmic signaling; (iv) PPAR ligand function *via* activation of intracellular signaling (*e.g.* the ERK cascade) by a PPAR-independent mechanism, which is derived from exogenous application of ligands binding to plasma membrane receptors (14). Until now, PPAR-dependent signaling pathways in steroidogenic testicular Leydig cells have not been studied.

The presence of G-coupled membrane estrogen receptor (GPER) has been reported in somatic cells of the male reproductive system and spermatozoa (15-19). This receptor mediates rapid estrogen signaling exclusively *via* several signaling molecules *e.g.* MAPK/ERK, cAMP, calcium ions (Ca^{2+}) or metalloproteinases (20). The role of GPER in control of endocrine tissue cell proliferation has been established (16, 21). Interestingly, recent findings revealed its function in lipid metabolism (22). Mice lacking GPER develop visceral obesity and show increased low density lipoproteins; however, the role and mechanisms of GPER signaling in lipid physiology remain undiscovered.

To address these issues, we examined the potential link between GPER and PPAR and if this interaction regulates steroidogenic function of mouse Leydig cells of varying ages. To further investigate the relationship of these receptors and elucidate specific effects of their interaction, MA-10 mouse tumor Leydig cells were utilized.

MATERIALS AND METHODS

Animals and treatments

Male mice (C57BL/6) 3 months-old (n = 10) and 2 years-old (n = 10) were obtained from Department of Genetics and Evolution, Institute of Zoology and Biomedical Research, Jagiellonian University in Cracow. Animals were maintained on 12 h dark-light (250 lux at cages level) cycle with stable temperature condition (22ºC), relative humidity of 55 ± 5% and free access to water and standard pelleted diet (LSM diet, Agropol, Motycz, Poland). Animals were killed by cervical dislocation.

All applicable international, national, and/or institutional guidelines for the care and use of animals were followed. The use of the animals was approved by the National Commission of Bioethics at the Jagiellonian University in Cracow, Poland (No. 151/2015).

Mice from various age groups were allotted into experimental groups (each group including 5 animals); control (Cont.) and treated receiving selective GPER receptor antagonist [(3a*S**,4*R**,9b*R**)-4-(6-Bromo-1,3-benzodioxol-5-yl)-3a,4,5,9b-3*H*-cyclopenta[c]quinolone; G-15] (Tocris Bioscience, Bristol, UK). G-15 was dissolved in DMSO and the stock solutions were kept at –20ºC. Animals from the experimental groups were injected subcutaneously with freshly prepared solutions of G-15 (50 μg/kg b.w.) in phosphate buffered saline (six doses each dose injected every other day). Mice from control groups received vehicle only. Dose, frequency and time of G-15 administration were based on literature data (23, 24) and it was finally selected upon our preliminary study in mice *in vivo* (doses range 5, 50, 100, 150, 200 μg/kg b.w.). Mice were sacrificed by cervical dislocation and testes were surgically removed.

Both testes of each individual of control and G-15-treated mice were surgically removed and were cut into small fragments. For immunohistochemistry, tissue samples were fixed in 10% formalin and embedded in paraffin. Small pieces of the testicular tissue were immediately frozen in a liquid nitrogen and stored at –80ºC for protein analysis. Blood was collected from liver vein and used for LH and cholesterol level measurements.

Cell culture and treatments

The mouse Leydig cell line MA-10 express luteinizing hormone/human chorionic gonadotropin (LH/hCG) receptors and display clear cAMP and steroidogenic response to gonadotropin stimulation as native Leydig cells. Due to the lack of 17α-hydroxylase expression, progesterone is the main steroid product in MA-10 cells (25, 26). MA-10 cells were a generous gift from Dr. Mario Ascoli (University of Iowa, Iowa City, IA), and were maintained under a standard technique (25). Middle passages of MA-10 cells were used for the study. The cells were grown in Waymouth's media (Gibco, Grand Island, NY) supplemented with 12% horse serum and 50 mg/l of gentamicin at 37ºC in 5% CO_2. Cells were plated overnight at a density of 1×10^5 cells/ml per well. Twenty-four hours before the experiments, the medium was removed and replaced with a medium without phenol red supplemented with 5% dextran-coated, charcoal-treated FBS (5% DC-FBS) to exclude estrogenic effects caused by the medium. Next, cells were treated with selective antagonists: GPER [(3a*S**,4*R**,9b*R**)-4-(6-Bromo-1,3-benzodioxol-5-yl)-3a,4,5,9b-3*H*-cyclopenta [c]quinolone; G-15] (Tocris Bioscience, Bristol, UK), PPARα [*N*-((2*S*)-2-(((1*Z*)-1-Methyl-3-oxo-3-(4-(trifluoromethyl) phenyl)prop-1-enyl)amino)-3-(4-(2-(5-methyl-2-phenyl-1,3-oxazol-4-yl)ethoxy)phenyl)propyl) propanamide, GW6471] or PPARγ [2-Chloro-5-nitro-*N*-4-pyridinylbenzamide, T0070907] freshly prepared as 100 nM stock solutions in dimethyl sulfoxide (DMSO) (Sigma-Aldrich) stored at –20ºC. A stock concentrations were subsequently dissolved in Waymouth's media a final concentrations. Cells were treated with G-15, PPARα or PPARγ alone or together for 24 hours. Doses of G-15 (10 nM), PPARα (10 μM) or PPARγ (10 μM) were based on literature data (27-33) and they were finally selected upon our preliminary studies (dose range 1, 10, 100 μM and 1, 10, 100 nM). We performed scanning microscopic analysis of Leydig cell phenotype and morphological structure (glutaraldehyde/formaldehyde-fixed) and fluorescence staining/immunocytochemistry (formadehyde/methanol and acetone-fixed). Cell lysates were frozen in –80ºC and used either for protein expression analyses or for cholesterol content measurement. Culture media were frozen in –20ºC for progesterone level determination.

Leydig cells *in vitro* and testes *in vivo* both control and treated with G-15, PPARα, PPARγ alone or in combinations were analyzed for expression and localization of fundamental

steroidogenesis controlling proteins (LHR, StAR, TSPO, PKA, P450scc, perilipin, HSL, HMGCR). Important goal of this study was also determination of signaling pathways molecules (Ras/Raf and PI3K/Akt) involved in GPER and PPAR partnership in control of cell physiology. Special consideration of Leydig cells topography and morpho-functionality was performed.

Western blot analysis

Lysates of testes of (control and treated with GPER antagonist) and Leydig cells (control and treated with GPER, PPARα, PPARγ antagonists alone or in combinations) were obtained by sample homogenization and sonication with a cold

Table 1. Primary antibodies used for immunocyto/histochemistry and Western blotting.

Antibody	Host species	Vendor	Dilution
GPER	Rabbit	Abcam cat. no. 39742	1:50 (ICC) 1:200 (IHC) 1:500 (WB)
PPARα	Mouse	Thermo Fisher Scientific cat. no. MA1-822	1:20 (ICC) 1:200 (IHC) 1:1000 (WB)
PPARγ	Rabbit	Abcam cat. no. 209350	1:50 (ICC) 1:400 (IHC) 1:500 (WB)
LHR (H-50)	Rabbit	Santa Cruz Biotechnology cat. no. sc-25828	1:10 (ICC) 1:500 (WB)
TSPO	Goat	Thermo Fisher Scientific cat.no. PA5-18565	1:50 (ICC) 1:250 (WB)
StAR	Mouse	Abcam cat. no. ab5813	1:50 (ICC) 1:500 (WB)
PKAIIβ	Rabbit	Santa Cruz Biotechnology cat. no. sc-25424	1:50 (ICC) 1:1000 (WB)
PLIN1	Rabbit	Cell Signaling Technology cat. no. 9349	1:200 (ICC) 1:500 (WB)
P450scc	Rabbit	Merck Millipore cat. no. ABS236	1:100 (ICC) 1:500 (WB)
HSL	Rabbit	Cell Signaling Technology cat. no. 4107	1:50 (ICC) 1:500 (WB)
HMGCR	Rabbit	Thermo Fisher Scientific cat.no. PA5-18565	1:50 (ICC) 1:1000 (WB)
Ras	Rabbit	Cell Signaling Technology cat. no. 3965	1:250 (WB)
t-Raf-1	Rabbit	Santa Cruz Biotechnology cat. no. sc-133	1:250 (WB)
PI3Kp85	Rabbit	Cell Signaling Technology cat. no. 4292	1:500 (WB)
t-Akt	Rabbit	Cell Signaling Technology cat. no. 9272S	1:500 (WB)
β-actin	Mouse	Sigma Aldrich cat. no. A2228	1:3000 (WB)

Abbreviations: GPER, G-coupled membrane estrogen receptor; PPARα, peroxisome proliferator-activated receptor α; PPARγ, peroxisome proliferator-activated receptor; LHR, lutropin receptor, TSPO, translocator protein; StAR, steroidogenic acute regulatory protein; PKA, protein kinase A; PLIN, perilipin; P450scc, cytochrome P450 side chain cleavage; HSL, hormone sensitive lipase; HMGCR, 3-hydroxy-3-methylglutaryl-CoA reductase; Ras, protein of small GTPase family; Raf, (rapidly accelerated fibrosarcoma) receptor tyrosine kinase effector; PI3K, phosphatidylinositol-4,5-bisphosphate 3-kinase; Akt-serine/threonine-specific protein kinase (Protein kinase B).

Tris/EDTA buffer (50 mM Tris, 1 mM EDTA, pH 7.5), supplemented with a broad-spectrum protease inhibitors (Sigma-Aldrich). The protein concentration was estimated by the Bio-Rad DC Protein Assay Kit with BSA as a standard (Bio-Rad Labs, GmbH, Munchen, Germany). Equal amounts of protein were resolved by SDS-PAGE under reducing conditions, transferred to polyvinylidene difluoride membranes (Merck Millipore, Darmstadt, Germany) and analyzed by Western blotting with antibodies listed in *Table 1*. The presence of the primary antibody was revealed with horseradish peroxidase-conjugated secondary antibodies diluted 1:3000 (Vector Lab., Burlingame, CA, USA) and visualized with an enhanced chemiluminescence detection system as previously described (19). All immunoblots were stripped with stripping buffer containing 62.5-mM Tris-HCL, 100-mM 2-mercaptoethanol, and 2% SDS (wt:v; pH 6.7) at 50ºC for 30 minutes, and incubated in antibody against *β*-actin (loading control). Three independent experiments were performed, each in triplicate with tissues prepared from different animals. To obtain quantitative results the bands (representing each data point) were densitometrically scanned using the public domain ImageJ software (National Institutes of Health, Bethesda, Maryland, USA) (34). The data obtained for each protein were normalized against its corresponding actin and expressed as relative intensity. Results of 10 separate measurements were expressed as mean ± SD.

Scanning electron microscope (SEM)

Leydig cells (control and treated with GPER, PPARα, PPARγ antagonists alone or in combinations), were fixed in a mixture of 2.5% glutaraldehyde with 2.5% formaldehyde in a 0.05 M cacodylate buffer (Sigma; pH 7.2) for 14 days, washed three times in a 0.1 M sodium cacodylate buffer and later dehydrated and subjected to critical-point drying. They were then sputter-coated with gold and examined at an accelerating voltage of 20 kV or 10 KV using a Hitachi S-4700 scanning electron microscope (Hitachi, Tokyo, Japan), which is housed in the Institute of Geological Sciences, Jagiellonian University in Cracow).

Cytoskeleton structure

Leydig cells (control and treated with GPER, PPARα, PPARγ antagonists alone or in combinations) were grown on coverslips (Ø12 mm; Menzel Glaeser, Germany). For the F-actin staining, the cells were fixed in 4% formaldehyde (freshly prepared from paraformaldehyde) in phosphate buffered saline (PBS) for 30 min at RT and stained with rhodamine-conjugated phalloidin (2 µg/ml, Sigma-Aldrich) for 40 min in darkness. Cells were mounted with Vectashield mounting medium (Vector Labs) with 40,6-diamidino-2-phenylindole (DAPI). Then, fluorescence was detected using epifluorescence microscope Leica DMR (Leica Microsystems).

For the microtubules localization, live cells were stained with Tubulin Tracker™ Oregon Green ® (Thermo Fisher Scientific) 500 µM in DMSO according to manufacturer's protocol. Cells were analyzed using epifluorescence microscope Leica DMR. The intensity of the fluorescence was calculated using a NIS-Elements software and expressed as relative fluorescence in a.u. (RFU). Results of 20 – 30 separate measurements of single cells from each experimental group were expressed as mean ± SD.

Alkaline phosphatase assay

Leydig cells (control and treated with GPER, PPARα, PPARγ antagonists alone or in combinations) were grown on coverslips. Alkaline phosphatase (ALP) activity was quantified by ELF 97 Endogenous Phosphatase Detection Kit (Molecular Probes, Eugene, OR). Briefly, cells were fixed in 3% formaldehyde for 10 minutes at room temperature. To permeabilize the cells, 200 µL/well of PBS/0.2% Tween-20 was added and the plates were incubated for 15 minutes. The cells were briefly rinsed twice in water, and then left for 10 minutes in H_2O. Substrate was diluted 1:20 in substrate buffer, 50 µL/well, and incubated for 5 minutes. Cells were mounted with DAPI. Fluorescence was detected using epifluorescence microscope Leica DMR. The intensity of the fluorescence was using a NIS-Elements software and expressed as relative fluorescence in a.u. (RFU). Results of 20 – 30 separate measurements of single cells from each experimental group were expressed as mean ± SD.

Immunohistochemistry and immunocytochemistry

To optimize immunohistochemical staining testicular sections both control and GPER antagonist-treated were immersed in 10 mM citrate buffer (pH 6.0) and heated in a microwave oven (2 × 5 min, 700 W). Thereafter, sections were immersed sequentially in H_2O_2 (3%; v/v) for 10 min and normal goat serum (5%; v/v) for 30 min which were used as blocking solutions. After overnight incubation at 4ºC with primary antibodies listed in *Table 1*. Next respective biotinylated antibodies (anti-rabbit, anti-goat and anti-mouse IgGs; 1: 400; Vector, Burlingame CA, USA) and avidin-biotinylated horseradish peroxidase complex (ABC/HRP; 1:100; Dako, Glostrup, Denmark) were applied in succession. Bound antibody was visualized with 3,3'-diaminobenzidine (DAB) (0.05 %; v/v; Sigma-Aldrich) as a chromogenic substrate. Control sections included omission of primary antibody and substitution by irrelevant IgG.

Immunocytochemistry was performed on Leydig cells (control and treated with GPER, PPARα, PPARγ antagonists alone or in combinations). Cells were fixed using absolute methanol for 7 minutes followed by acetone for 4 minutes both at –20ºC respectively. Next, cells were rinsed in TBS containing 0.1% Triton X-100. Nonspecific binding sites were blocked with 5% normal goat or horse serum for 30 minutes. Thereafter, cells were incubated overnight at 4ºC in a humidified chamber in the presence of primary antibodies listed in *Table 1*. On the next day, biotinylated antibody goat anti-rabbit or horse anti-mouse (1:400; Vector Laboratories) were applied for 60 minutes, respectively. After each step in these procedures, cells were carefully rinsed with TBS; the antibodies were also diluted in TBS buffer. The staining was developed using ABC⁄HRP complex for 30 minutes followed by DAB. Thereafter, cells were washed, and some of them were counterstained with Mayer's hematoxylin and mounted using DPX mounting media (Sigma-Aldrich). Cells were examined with Leica DMR microscope (Leica Microsystems, Wetzlar, Germany). The whole procedure was described in detail elsewhere (19, 35, 36). Experiments were repeated three times. To evaluate the intensity of immunohistochemical reaction quantitatively, digital images were obtained and analyzed using a NIS-Elements software and expressed as relative optical density (ROD) of DAB brown reaction products. Results of 20 – 30 separate measurements of bands on different blots were expressed as mean ± SD.

ELISA assays

Mouse Luteinizing Hormone Elisa Kit (Biocompare, San Francisco, USA) was used for examination of LH concentrations in serum of control and GPER antagonist-treated mice according to the manufacturer's instructions. The sensitivity of the assay

was 0.1 mIU/ml. The absorbance (λ = 450 nm) was measured. Data were expressed as mean ± SD.

Progesterone Enzyme Immunoassay Kit (DRG, Marburg, Germany) was used for measurement of progesterone content in culture media in control and treated with GPER, PPARα, PPARγ antagonists (alone or in combinations) Leydig cells according to the manufacturer's instructions. The sensitivity of the assay was 0.045 ng/mL. The absorbance (λ = 480 nm) was measured. Data

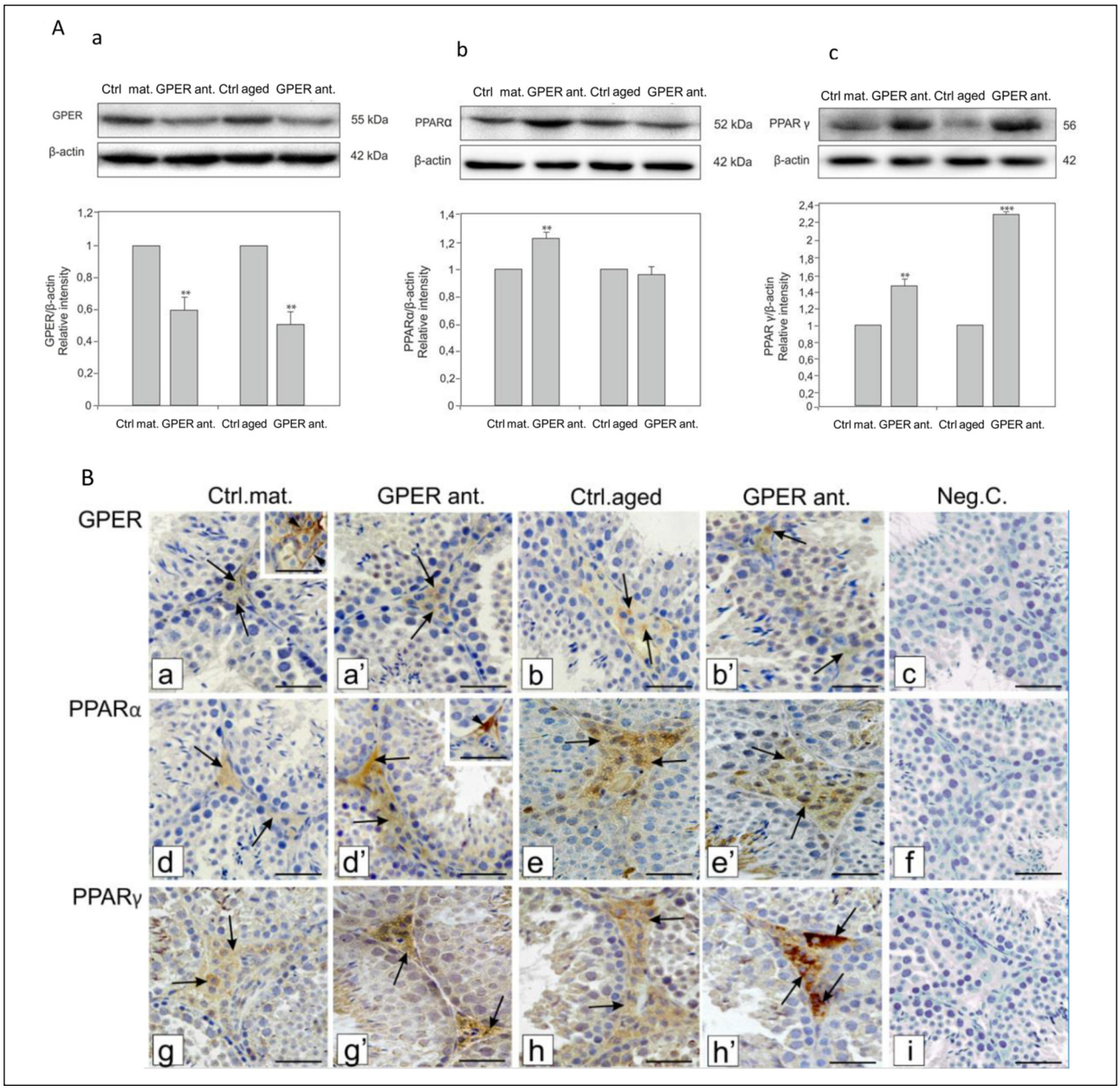

Fig. 1. Effect of GPER blockage on expression and localization of GPER, PPARα and PPARγ in mouse testes.
(A) Representative blots of qualitative expression of GPER (a), PPARα (b), and PPARγ (c) and relative expression (relative quantification of protein density (ROD); arbitrary units). The relative amount of respective proteins normalized to β-actin. ROD from three separate analyses is expressed as means ± SD. Asterisks show significant differences between respective control mature and aged mouse testes and those treated with GPER antagonist (50 µg/kg b.w.). Values are denoted as *P < 0.05, **P < 0.01 and ***P < 0.001. From each animal at least three samples were measured.
(B) Representative microphotographs of cellular localization of GPER (a, a', b, b'), PPARα (c', d, d', e, e') and PPARγ (f, f', g, g') in testes of control mature and aged mice and those treated with GPER antagonist (50 µg/kg b.w.). DAB immunostaining with hematoxylin counterstaining. Scale bars represent 15 µm. From each animal 3 – 5 serial testicular sections were analyzed. (a, b) GPER protein is visible in membrane and cytoplasm (insert at a) of Leydig cells of control mature and aged testes (arrows). Moderate intensity of immunoreaction is seen in control testes of both age groups while it is very weak in Leydig cells of those GPER ant.-treated (arrows) (a', b'). Independent of animal age, expression of PPARα in cytoplasm of Leydig cells either of control or experimental testes is visible (d, d', e, e'). No significant changes in immunoreaction intensity for PPARα are observed with exception of Leydig cells of mature GPER ant.-treated testes (arrows) (d'). In this case strong reaction is observed in individual cells (insert at d'). Positive signal for PPARγ is noted in cytoplasm of control and GPER ant.-treated males (arrows) (f, f', g, g'). Note, the strongest reaction in GPER ant.-treated testes both mature and aged (arrows) (f', g'). In negative controls no immunostaining is found (c, f, i).

were expressed as mean ± SD. The measurements were performed with the use microplate reader (Labtech LT-4500).

Cholesterol assay

The Amplex® Red Cholesterol Assay Kit (Molecular Probes Inc., Eugene, OR, USA) was used for cholesterol content (μM) analysis in control and GPER antagonist-treated males and Leydig cells treated with GPER, PPARα, PPARγ antagonists alone or in combinations. For measurement 100 μl cell lysates was used according to manufacturer' s protocol. Data were expressed as mean ± SD. The fluorescence (λ = 580 nm) was measured with the use of a fluorescence multiwell plate reader SPARK Tecan, Switzerland.

Migration assay

QCM™ Chemotaxis 96-well Cell Migration Assay (Chemicon Incorporation Int.) was performed in control and GPER, PPARα, PPARγ antagonists-treated Leydig cells (alone or in combinations) according manufacturer's instruction. The fluorescence (λ = 480 nm) was measured with the use of a fluorescence multiwell plate reader SPARK Tecan, Switzerland. Data (relative fluorescence units; RFU) were expressed as mean ± SD.

Statistical analysis

Each variable was tested by using the Shapiro-Wilk W-test for normality. Homogeneity of variance was assessed with Levene's test. Since the distribution of the variables was normal and the values were homogeneous in variance, all statistical analyses were performed using one-way analysis of variance (ANOVA) followed by Tukey's *post hoc* comparison test to determine which values differed significantly from controls. The analysis was made using Statistica software (StatSoft, Tulsa, OK, USA). Data were presented as mean ± SD. Data were considered statistically significant at $P<0.05$. All the experimental measurements were performed in triplicate.

RESULTS

Effect of GPER blockage on expression and localization of GPER, PPARα and PPARγ in mouse testes

In mice treated with GPER antagonist, decreased GPER expression was observed ($P < 0.01$) (*Fig. 1A*). Different alterations of PPAR expression were found in GPER blocked mice. Expression of PPARα was increased ($P < 0.001$) in mature males while it remained unchanged in aged ones when compared to controls. In contrast, expression of PPARγ was increased in both treated groups ($P < 0.01$, $P < 0.001$).

The GPER protein was localized to the cell membrane (insert at a) and cytoplasm of Leydig cells of control, mature, and aged testes (*Fig. 1Ba* and *1Bb*). Expression was of moderate intensity, while it was very weak in Leydig cells of mature and aged testis upon GPER antagonist treatment (*Fig. 1Ba'* and *1Bb'*). Regardless of the animal age, PPARα expression was observed in Leydig cell cytoplasm of control and experimental testes (*Fig. 1Bd*, *1Be* and *1Bd'*, *1Be'*). No significant changes in immunoreaction intensity were found in Leydig cells with the exception of mature GPER antagonist-treated testes. In this case, a strong reaction was observed in individual cells (insert at d'). A positive signal for PPARγ was found in the cytoplasm of control and GPER-treated testes both control and experimental (*Fig. 1Bf*, *1Bf'* and *1Bg*, *1Bg'*). The strongest reaction was always observed in Leydig cells of GPER antagonist-treated mature and aged males (*Fig. 1Bf'* and *1Bg'*). In negative controls, no immunostaining was observed (*Fig. 1Bc*, *1Bf* and *1Bi*).

Effect of GPER blockage on LHR, StAR, and TSPO expression in mouse testes

After exposure to the GPER antagonist, LHR expression was increased in mature and aged testes ($P < 0.01$, $P < 0.001$) when compared to their respective controls (*Fig. 2a*). Expression of StAR was markedly increased only in mature -GPER antagonist treated males ($P < 0.001$) while it remained unchanged in aged animals (*Fig. 2b*). A significant increase in TSPO expression was

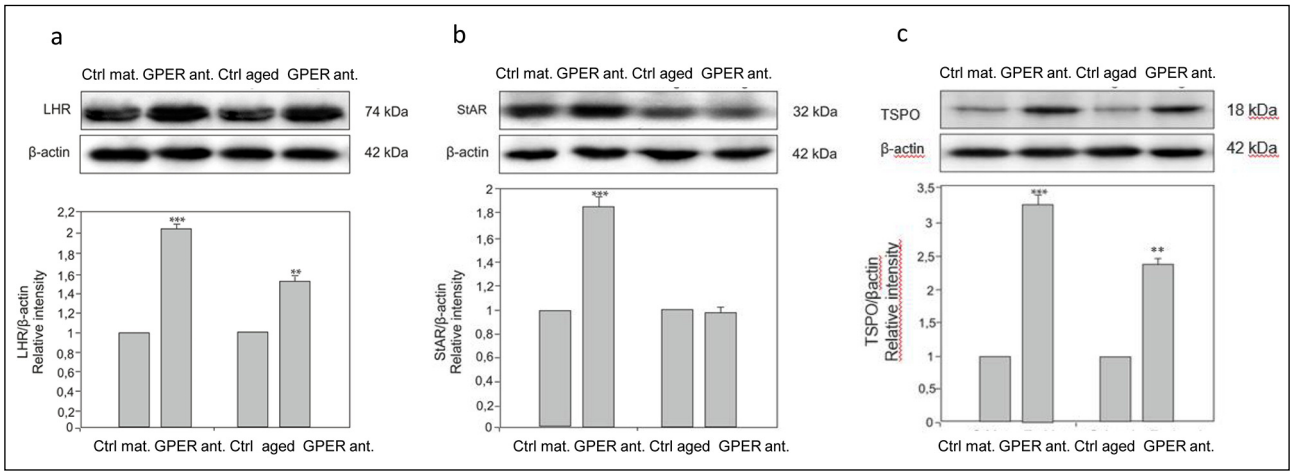

Fig. 2. Effect of GPER blockage on expression of LHR, StAR, TSPO in mouse testes.
(A) Representative blots of qualitative expression of LHR (a), StAR (b), and TSPO (c) and relative expression (relative quantification of protein density (ROD); arbitrary units). The relative amount of respective proteins normalized to β-actin. ROD from three separate analyses is expressed as means ± SD. Asterisks show significant differences between respective control mature and aged testes and those treated with GPER ant. (50 μg/kg b.w.). Values are denoted as $**P < 0.01$ and $***P < 0.001$. From each animal at least three samples were measured.

found in both mature and aged testes ($P < 0.01$, $P < 0.001$) (*Fig. 2c*).

Effect of GPER blockage on lutropin concentration in mouse serum

In serum of control mice, increased LH levels were observed in aged animals as compared to mature mice ($P < 0.01$, $P < 0.001$) (*Fig. 3A*). Exposure to the GPER antagonist increased LH levels markedly in both groups of treated mature and aged mice, respectively ($P < 0.05$, $P < 0.001$).

Effect of GPER blockage on cholesterol content in mouse testes

Cholesterol content in mature male testes was lower than in aged ones ($P < 0.05$) (*Fig. 3B*). After GPER antagonist treatment, cholesterol content decreased in both groups ($P < 0.05$, $P < 0.01$).

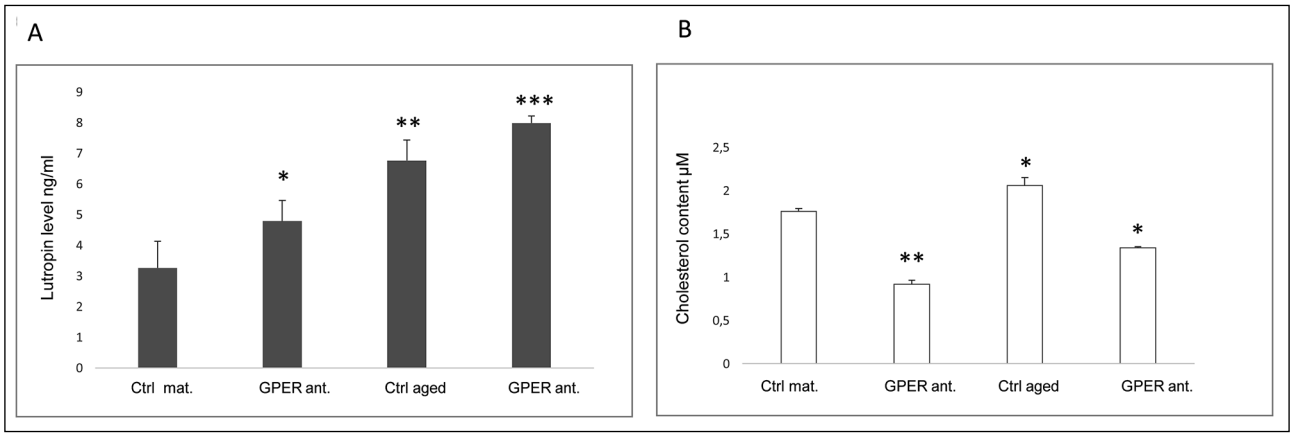

Fig. 3. Effect of GPER blockage on lutropin concentration in serum and cholesterol content in testes of mice. Serum lutropin concentration (A) and cholesterol content in testes (B) of control mature and aged mice and those treated with GPER ant. (50 µg/kg b.w.). Values are denoted as $*P < 0.05$, $**P < 0.01$ and $***P < 0.001$. From each animal at least three samples were measured.

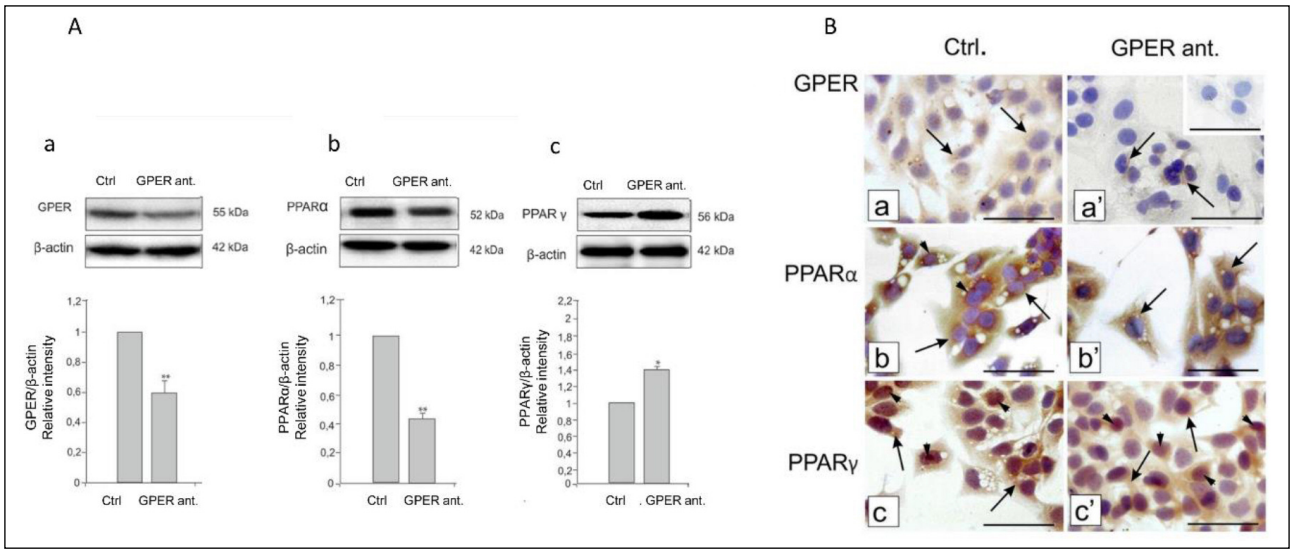

Fig. 4. Effect of GPER blockage on expression and localization of PPARα and PPARγ in mouse Leydig cells.
(A) Representative blots of qualitative expression of GPER (a), PPARα (b), and PPARγ (c) and relative expression (relative quantification of protein density (ROD); arbitrary units). The relative amount of respective proteins normalized to β-actin. ROD from three separate analyses is expressed as means ± SD. Asterisks show significant differences between control and treated with GPER (10 nM) for 24 h Leydig cells. Values are denoted as $*P < 0.05$, $** P < 0.01$. For analysis at least three cell samples were measured.
(B) Representative microphotographs of cellular localization of GPER (a, a), PPARα (b, b') and PPARγ (c, c') in control and GPER ant. (10 nM) Leydig cells treated for 24 h. DAB immunostaining with hematoxylin counterstaining. Scale bars represent 15 µm. For immunostaining at least three cell cultures control and experimental were used. In control and GPER ant.-treated Leydig cells very week, cytoplasmic staining for GPER is seen (arrows) (a, a'). Note, no changes in localization and expression of both PPAR receptors in control and treated cells (b, b' and c, c'). Cytoplasmic (arrows) and perinuclear (arrowheads) expression of PPARα is strong in both control and GPER ant.-treated cells (b, b'). PPARγ is localized either in cytoplasm (arrows) or in nucleus (arrowheads) in control and GPER ant.-treated cells. No changes in PPARγ immunostaining intensity are observed (c, c'). In negative controls no immunostaining is found (representative insert at a').

Effect of GPER blockage on expression and localization of PPARα and PPARγ in mouse Leydig cells

In Leydig cells, GPER antagonist treatment decreased immunoexpression of GPER (*Fig. 4Aa*). After GPER antagonist treatment, the opposite effect was found on PPARα and PPARγ expression (*Fig. 4Ab* and *4Ac*). Immunoexpression of PPARα was decreased ($P < 0.01$) while those of PPARγ was increased ($P < 0.05$) in comparison to control.

In control and GPER antagonist-treated Leydig cells, very weak cytoplasmic GPER staining was found (*Fig. 4Ba* and *4Ba'*). No marked changes in localization and expression of both PPARα and PPARγ were revealed between control and GPER antagonist-treated cells (*Fig. 4Bb*, *4Bb'* and *4Bc*, *4Bc'*). Cytoplasmic expression of PPARα was strong in both control and GPER antagonist-treated cells (Fig. *4Bb* and *4Bb'*). In controls, PPARα staining was localized especially in the perinuclear region of cells. PPARγ was present either in the cytoplasm or nucleus of control and GPER antagonist-treated cells. The strongest expression of PPARγ was always seen in control cells versus treated. In negative controls, no immunostaining was found (*Fig. 4B* representative insert at a').

Effect of GPER, PPARα, and PPARγ blockage on mouse Leydig cell morphology

Scanning electron microscopic analysis revealed a normal structure of control Leydig cells (*Fig. 5Aa*). Cells grew as a monolayer and were well-adhered to the bottom of the dish. A majority of cells showed a polygonal shape with small and short pseudopodia. Regardless of antagonist used (PPARα, PPARγ not shown) alone or in combination, alterations in cell shape were observed (*Fig. 5Ab-5Ae*). A great number of elongated Leydig cells possessing long pseudopodia was observed. On the cell surface, small microvilli were seen, particularly in cells treated with antagonists (*Fig. 5Af* and *5Ag*). After treatment, proliferating cells were commonly seen (*Fig. 5Ag* and *5Ah*).

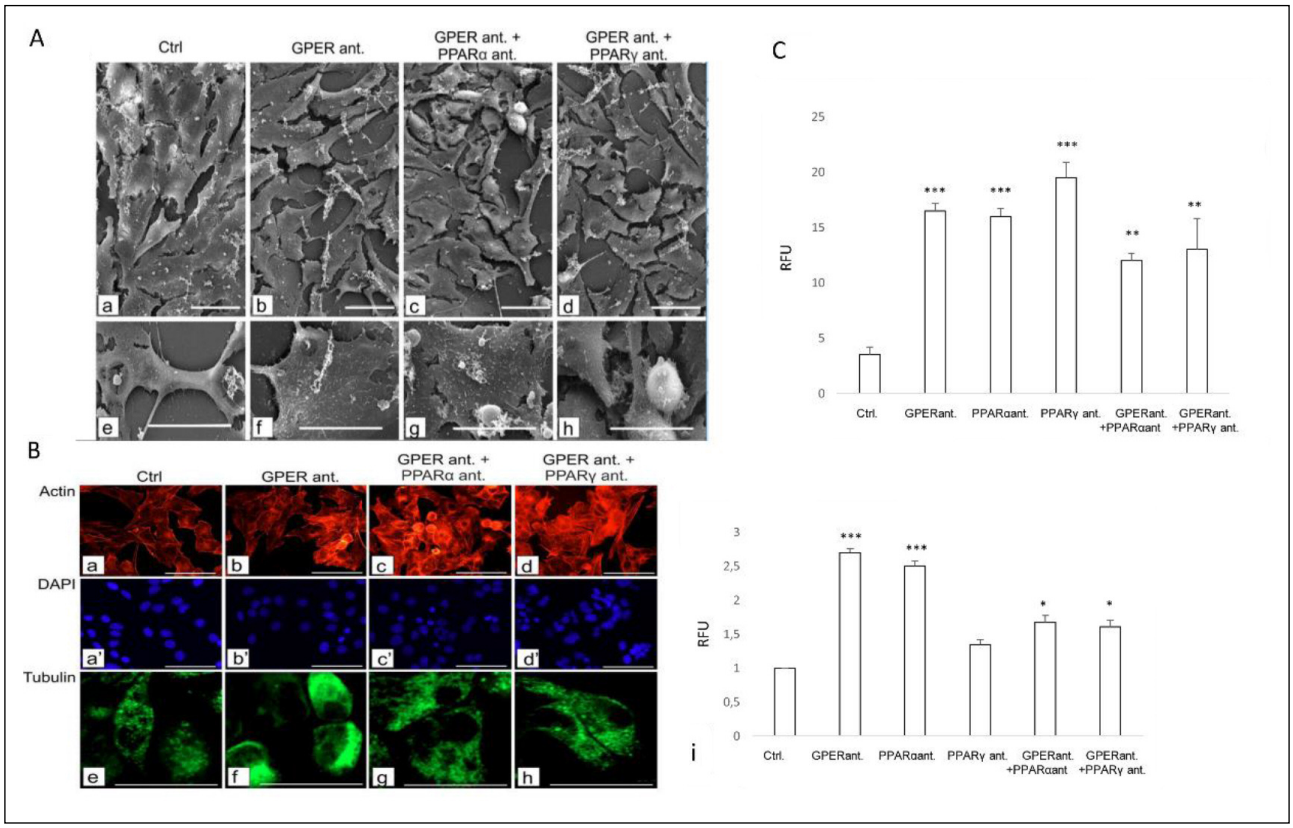

Fig. 5. Effect of GPER, PPARα and PPARγ blockage on morphology of mouse Leydig cells.
(A) Representative microphotographs of scanning electron microscopic analysis of control, GPER (10 nM), PPARα (10 μM), PPARγ (10 μM) antagonists-treated Leydig cells (a-h). Bars represent 1 μm. For analysis at least three control and experimental cell cultures were used. Normal structure of control Leydig cells (a). Cells are growing in monolayer, and are well-adhered to the dish bottom. Majority of cells show polygonal shape with small and short pseudopodia. Note, changes in cell shape after treatment with antagonists; GPER and PPARα, PPARγ alone (not shown) or in combination (b-d, e). Great number of elongated Leydig cells possessing several, long pseudopodia is observed. In treated cells, on the cell surface number of small microvilli is seen (f, g). After treatment proliferating cells are commonly seen (g, h).
(B) Representative microphotographs of actin (a-d) and tubulin (e-h) activity in control and treated with GPER (10 nM), PPARα (10 μM) and PPARγ (10 μM) antagonists Leydig cells for 24 h. Fluorescence with DAPI for actin and without for tubulin staining. Scale bars represent 15 μm. (i) Histograms of tubulin expression of control and GPER (10 nM), PPARα (10 μM), PPARγ (10 μM) antagonists-treated Leydig cells. Fluorescence measured in relative fluorescence arbitrary units (RFU) from three separate analyses is expressed as means ± SD. Values are denoted as $*P < 0.05$ and $***P < 0.001$. For analysis at least three control and experimental cell cultures were used.
(C) Histograms of migration competences of control and GPER (10 nM), PPARα (10 μM), PPARγ (10 μM) antagonists-treated Leydig cells. Immunofluorescence measured in relative fluorescence arbitrary units (RFU) from three separate analyses is expressed as means ± SD. Values are denoted as $**P < 0.01$ and $***P < 0.001$.

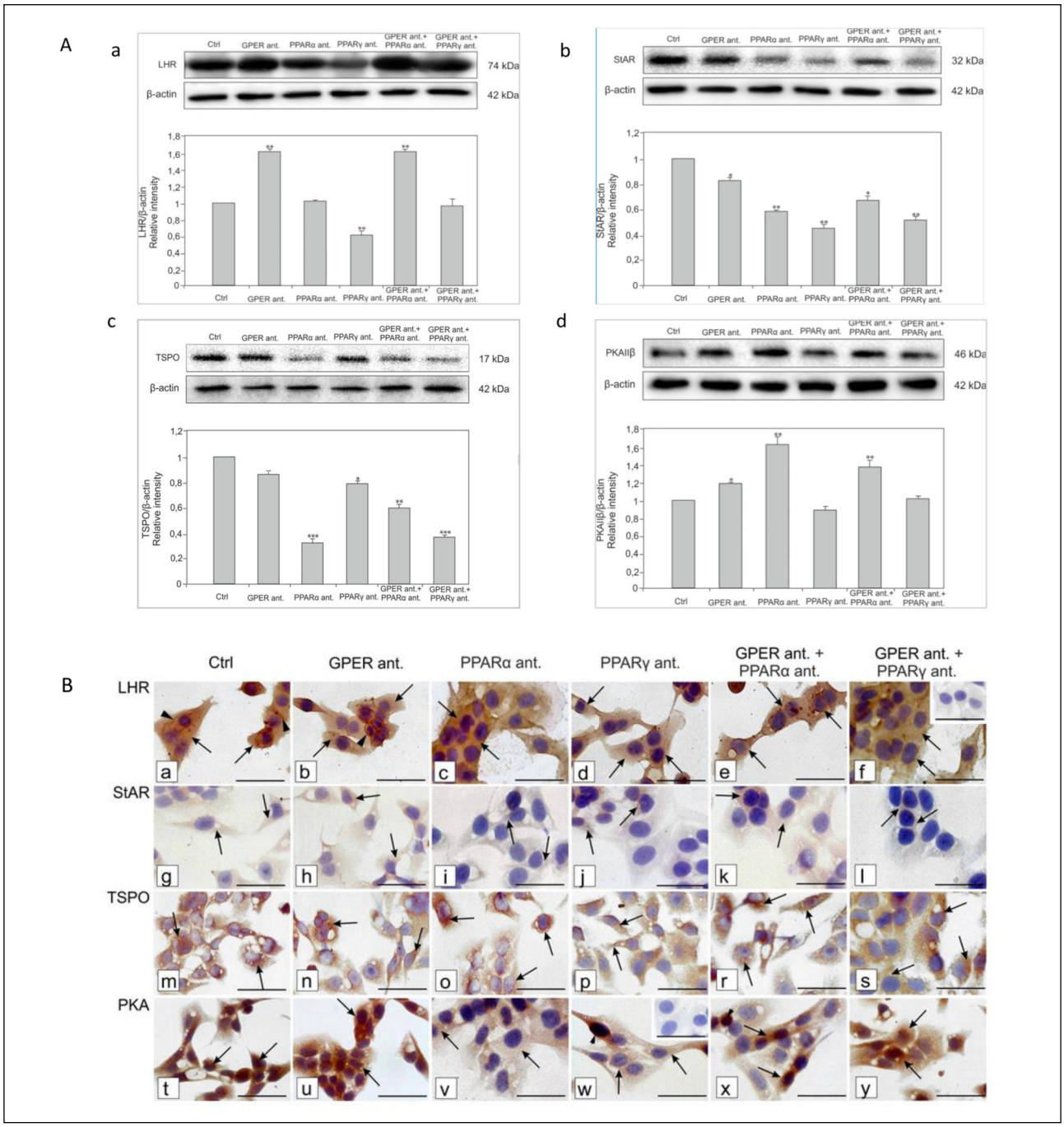

Fig. 6. Effect of GPER, PPARα and PPARγ blockage on expression and localization of steroidogenic LHR, StAR, TSPO, PKA proteins in mouse Leydig cells.

(A) Representative blots of qualitative expression of LHR (a), StAR (b), TSPO (c) and PKA (d) and relative expression (relative quantification of protein density (ROD); arbitrary units). The relative amount of respective proteins normalized to β-actin. ROD from three separate analyses is expressed as means ± SD. Asterisks show significant differences between control and treated with GPER (10 nM), PPARα (10 μM) and PPARγ (10 μM) antagonists Leydig cells for 24 h. Values are denoted as *P < 0.05, **P < 0.01, ***P < 0.001. For analysis at least three cell samples were measured.

(B) Representative microphotographs of cellular localization of LHR (a-f), StAR (g-l), TSPO (m-s) and PKA (t-y) in control and treated with GPER (10 nM), PPARα (10 μM) and PPARγ (10 μM) antagonists Leydig cells for 24 h. DAB immunostaining with hematoxylin counterstaining. Scale bars represent 15 μm. For immunostaining at least three control and experimental cell cultures were used.

Note no changes in staining intensity and localization of LHR and StAR between control and treated with antagonists Leydig cells (a-f and g-l). Immunoexpression of LHR is strong and visible in cell cytoplasm (arrows) and membrane (arrowheads, in control and GPER ant.-treated cells), while that of StAR is very week and visible exclusively in cell cytoplasm (arrows) (a-f, g-l). Immunostaining for TSPO is seen in cytoplasm (arrows) and in perinuclear region (arrowheads) of control and treated cells (m-s). Its immunoexpression is of weak to moderate intensity. Different expression of PKA after treatment of cells with PPARα and PPARγ antagonist alone or together with GPER is observed (t-y). Cells treated with PPARα and PPARγ alone show weak, cytoplasmic expression of PKA while it is of moderate intensity after each of PPAR antagonists added with GPER antagonist (arrows). In control and GPER ant.-treated cells PKA expression is very strong (arrows). In negative controls no immunostaining is found (representative insert at f).

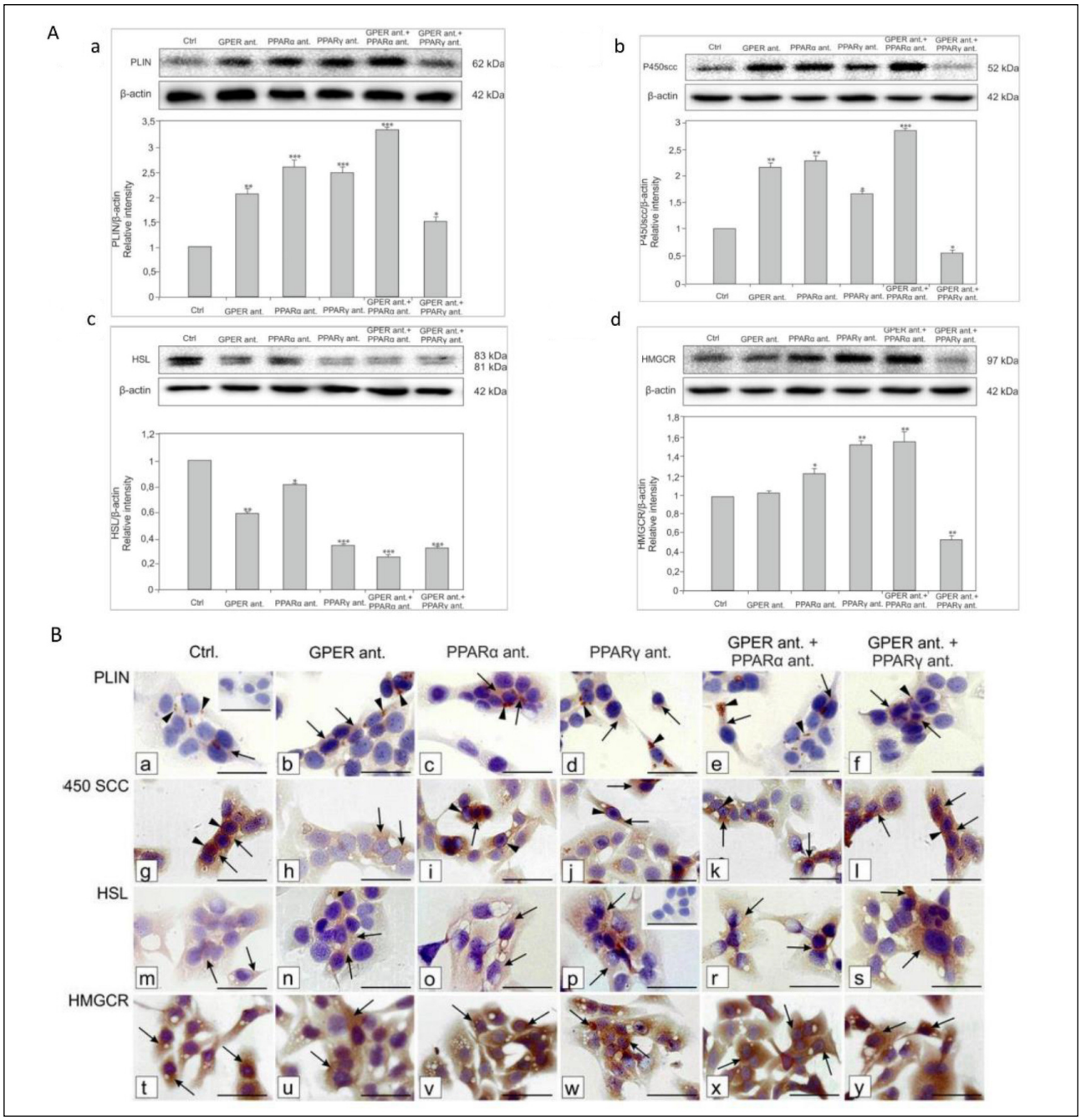

Fig. 7. Effect of GPER, PPARα and PPARγ blockage on expression and localization of steroidogenic PLIN, P450scc, HMGCR proteins in mouse Leydig cells.

(A) Representative blots of qualitative expression of PLIN (a), P450scc (b), HSL (c) and HMGCR (d) and relative expression (relative quantification of protein density (ROD); arbitrary units). The relative amount of respective proteins normalized to β-actin. ROD from three separate analyses is expressed as means ± SD. Asterisks show significant differences between control and treated with GPER (10 nM), PPARα (10 μM) and PPARγ (10 μM) antagonists Leydig cells for 24 h. Values are denoted as *P < 0.05, **P < 0.01, ***P < 0.01. For analysis at least three cell samples were measured.

(B) Representative microphotographs of cellular localization of PLIN (a-f), P450scc (g-l), HSL (m-s) and HMGCR (t-y) in control and treated with GPER (10 nM), PPARα (10 μM) and PPARγ (10 μM) antagonists Leydig cells for 24 h. DAB immunostaining with hematoxylin counterstaining. Scale bars represent 15 μm. For immunostaining at least three control and experimental cell cultures were used.

Positive staining for PLIN is present around lipid droplets (arrowheads) and in cytoplasm (arrows) in all analyzed cells (control and experimental ones) (arrows) (a-f). Note no significant changes in immunostaining intensity between control and experimental groups. Cytoplasmic (arrows) and perinuclear (arrowheads) reaction for P450scc is seen in control and cells-treated with antagonists (g-l). The intensity of staining is strong in all treated groups, without those PPARγ ant. and GPER ant.-treated, that is comparable to control. The weakest expression of HSL is found in cytoplasm of cells treated with PPARγ and GPER ant. while it is unchanged in other treated cell groups including control (arrows) (m-s). No changes in localization pattern and the strongest expression among studied proteins are observed for HMGCR (t-y). The enzyme is located in cytoplasm of control and treated cells (arrows). In negative controls no immunostaining is found (representative insert at P).

Significant amounts of actin filaments were seen in cortical regions of control cells (*Fig. 5Ba*). The cells sent numerous actin-rich pseudopodium-like protrusions after treatment with GPER, PPARα, or PPARγ alone (PPARα, PPARγ not shown) or in combination (*Fig. 5Bb-5Bd*). Additionally, actin associated with cell cortices and pseudopodium-like protrusion were observed as short and very thin filiform or finger-like projections with abundant F-actin bundles.

Microtubules composed of tubulin particles were present in both control and treated cells; however, in the latter, their presence was increased (*Fig. 5Be-5Bh*). Expression of tubulin increased significantly ($P < 0.05$, $P < 0.001$) in cells treated with GPER, PPARα, or PPARγ alone (PPARα, PPARγ not shown only at microphotographs) or in combination (*Fig. 5Be-5Bh* and *5Bj*).

The migration assay revealed increased ($P < 0.01$, $P < 0.001$) migration competences of Leydig cells treated with antagonists, alone and in combination, when compared to controls (*Fig. 5C*). Combined treatment resulted in increased migration competences versus treatment with each antagonist separately.

Effect of GPER, PPARα, and PPARγ blockage on expression and localization of steroidogenic LHR, StAR, TSPO, PKA and P450scc, PLIN, HMGCR as well as signaling Ras, Raf, PI3K, and Akt proteins in mouse Leydig cells

Expression of LHR in Leydig cells increased ($P < 0.01$) after treatment with GPER antagonist alone or in combination with PPARα or PPARγ antagonist (*Fig. 6Aa*). Only treatment with the PPARγ antagonist significantly decreased LHR expression ($P < 0.01$) while treatment with a PPARα antagonist had no effect (*Fig. 6Aa*). Treatment with PPARα and PPARγ antagonist alone or in combinations with GPER antagonist markedly decreased ($P < 0.01$, $P < 0.001$) StAR expression (*Fig. 6Ab*). Similarly, the most notable decrease ($P < 0.05$, $P < 0.01$, $P < 0.001$) in TSPO expression was revealed after Leydig cell treatment with PPAR antagonists alone or together with the GPER antagonist. Treatment with the GPER antagonist caused a subtle decrease in TSPO expression (*Fig. 6Ac*). PKA expression was increased ($P < 0.01$, $P < 0.001$) in all treated Leydig cell groups except for the PPARγ antagonist-treated one, where it was slightly decreased (*Fig. 6Ad*).

In control cells and those treated with GPER, PPARα, and PPARγ antagonists, separately or together, no marked changes in localization and immunostaining for LHR, StAR, and TSPO were found (*Fig. 6Ba-6Bf*, *6Bg-6Bl*, *6Bm-6Bs*). LHR expression was pronounced and found to be localized in the cytoplasm and cell membrane, while StAR expression was very weak and present exclusively in the cytoplasm (*Fig. 6Ba-6Bf* and *6Bg-6Bl*). TSPO was found in the cytoplasm, particularly in the perinuclear region of cells (*Fig. 6Bm-6Bs*), and its immunoexpression was of weak to moderate intensity. A slight increase in TSPO expression was seen in cells treated with GPER and PPARα together (*Fig. 6Bs*). Changes in immunostaining were observed for PKA (*Fig. 6Bt-6By*) after

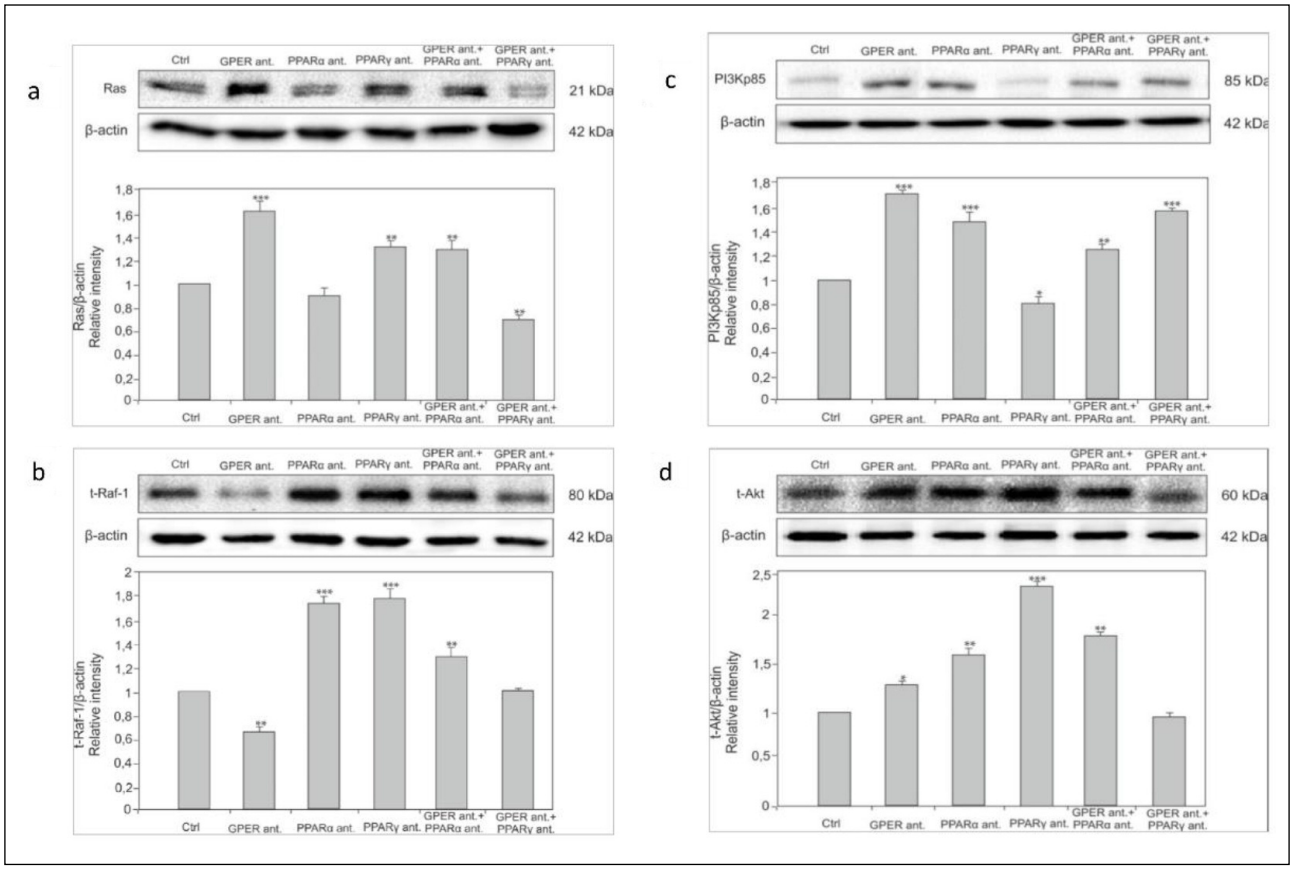

Fig. 8. Effect of GPER, PPARα and PPARγ blockage on expression and localization of signaling Ras, Raf, PI3K, Akt proteins in mouse Leydig cells.
(A) Representative blots of qualitative expression of Ras (a), Raf (b), PI3K (c) and Akt (d) and relative expression (relative quantification of protein density (ROD); arbitrary units). The relative amount of respective proteins normalized to β-actin. ROD from three separate analyses is expressed as means ± SD. Asterisks show significant differences between control and treated with GPER (10 nM), PPARα (10 μM) and PPARγ (10 μM) antagonists Leydig cells for 24 h. Values are denoted as *$P < 0.05$, **$P < 0.01$, ***$P < 0.01$. For analysis at least three cell samples were measured.

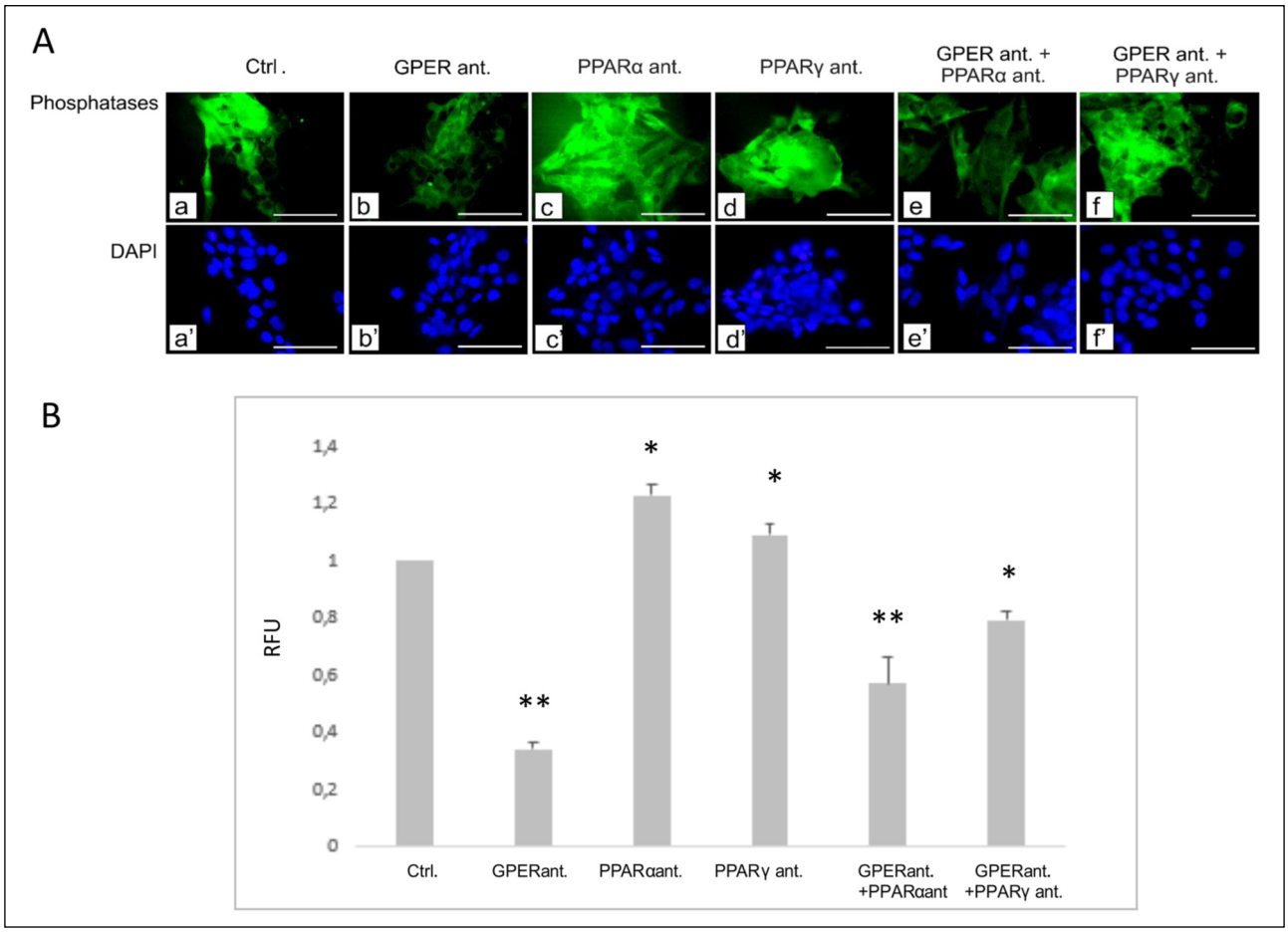

Fig. 9. Effect of GPER, PPARα and PPARγ blockage on phosphatases expression in mouse Leydig cells.
(A) Representative microphotographs of phosphatases activity in control and treated with GPER (10 nM), PPARα (10 μM) and PPARγ (10 μM) antagonists Leydig cells for 24 h.
Immunofluorescence with DAPI. Bars represent 20 μm. For analysis at least three control and experimental cell cultures were used.
(B) Histograms of immunofluorescence staining intensities analyses (RFU) from three separate analyses is expressed as means ± SD. Values are denoted as *P < 0.05, **P < 0.01, ***P < 0.01.

treatment of cells with PPARα and PPARγ antagonists alone or together with GPER (*Fig. 6Bu*, *6Bv*, *6Bx* and *6By*). Cells treated with PPARα and PPARγ alone showed weak cytoplasmic expression of PKA (*Fig. 6Bv* and *6Bw*). In control and GPER antagonist-treated cells, PKA expression was strong (*Fig. 6Bt* and *6Bu*). In negative controls, no immunostaining was found (*Fig. 6B* representative insert at *f*).

Following treatment with any of the antagonists, alone or in combination, increased ($P < 0.05$, $P < 0.01$, $P < 0.001$) PLIN expression in all treated groups was revealed (*Fig. 7Aa*). Similar changes were observed with P450scc expression (*Fig. 7Ab*) as it increased ($P < 0.05$, $P < 0.01$, $P < 0.001$) in all treated Leydig cell groups with the exception of cells treated with PPARγ and GPER antagonists, where it was subsequently decreased ($P < 0.05$). Expression of HSL decreased ($P < 0.05$, $P < 0.01$, $P < 0.001$) in all treated groups (*Fig. 7Ac*). The decrease was most pronounced in cells treated with the PPARα antagonist. Expression of HMGCR showed no changes after GPER antagonist treatment. However, it was increased ($P < 0.05$, $P < 0.01$) in all treated cell groups, but not in those treated with PPARγ and GPER antagonists, where it was decreased ($P < 0.01$) (*Fig. 7Ad*).

PLIN was localized around lipid droplets and occasionally in the cytoplasm in both control and experimental cells (*Fig. 7Ba-7Bf*). No significant changes in immunostaining intensity were found between the groups. Immunoreaction for P450scc was found both in cytoplasm and perinuclear region in control and cells treated with antagonists alone or in combination (*Fig. 7Bg-7Bl*). Staining intensity was strong in all treated groups, but after PPARγ GPER antagonists it was comparable to control cells. Similarly, expression of HSL was weakest in the cytoplasm of cells treated with PPARγ and GPER antagonists but was unchanged in other treated cell groups, including controls (*Fig. 7Bm-7Bs*). No changes in localization pattern of HMGCR were observed, and it had the strongest expression among studied proteins (*Fig. 7Bt-7By*). The enzyme was located in the cytoplasm of control and treated cells. In negative controls, no immunostaining was found (*Fig. 7B* representative insert at p).

Expression of Ras was altered ($P < 0.01$, $P < 0.001$) in GPER, PPARγ, and PPARα antagonist-treated cells (*Fig. 8a*). No changes in Ras expression were found in cells treated with the PPARα antagonist. Using the PPARγ and GPER antagonist, Ras levels were decreased ($P < 0.01$). Expression of Raf was decreased ($P < 0.01$) after GPER antagonist while it was increased ($P < 0.01$, $P < 0.001$) in other experimental groups with exception of PPARγ ant.- and GPER ant.-treated cells where it remained unchanged (*Fig. 8b*). Increased ($P < 0.01$, $P < 0.001$) expression of PI3K was found in treated cells independent of antagonist and treatment combination used, but not in cells treated with PPARγ antagonist and GPER antagonist where it

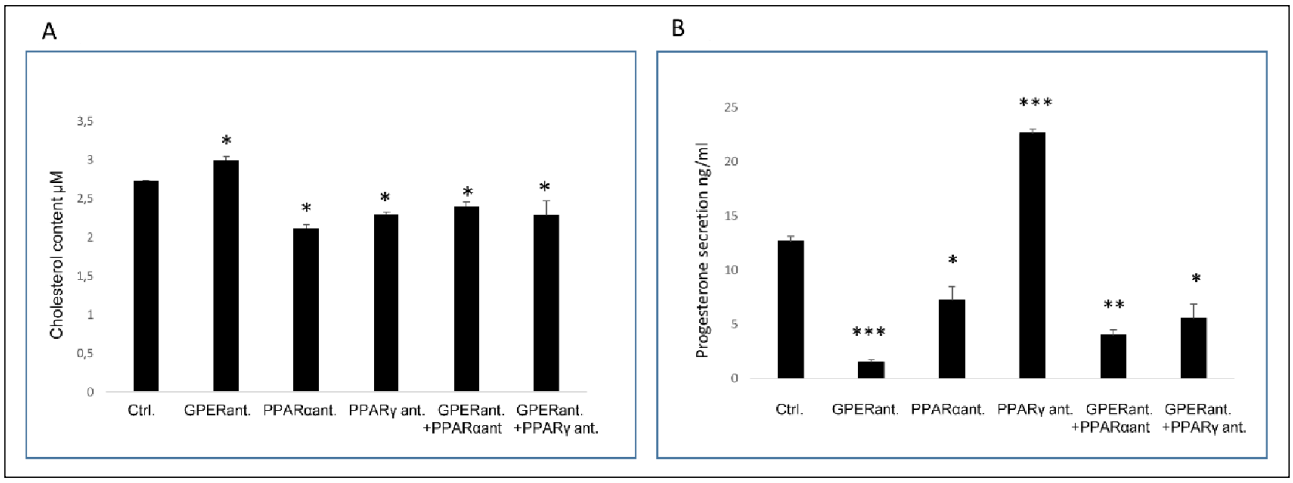

Fig. 10. Effect of GPER, PPARα and PPARγ blockage on cholesterol content and progesterone secretion by mouse Leydig cells. Cholesterol content (A) and progesterone secretion (B) in control and treated with GPER (10 nM), PPARα (10 μM) and PPARγ (10 μM) antagonists Leydig cells for 24 h. Values are denoted as *P < 0.05, **P < 0.01, and ***P < 0.001. For analysis at least three control and experimental cell cultures were used.

was decreased (P < 0.05) (*Fig. 8c*). Expression of Akt was increased (P < 0.05, P < 0.01, P < 0.001) in all treated groups apart from PPARγ and GPER antagonist-treated cells, where expression was unchanged (*Fig. 8d*).

Effect of GPER, PPARα, and PPARγ blockage on phosphatase expression in mouse Leydig cells

In Leydig cells, phosphatase levels significantly decreased following exposure to the GPER (P < 0.01) (*Fig. 9*). Treatment with both PPAR antagonists increased (P < 0.05) expression of phosphatases while concomitant treatment with each of PPAR antagonists and GPER decreased (P < 0.05, P < 0.01) phosphatase expression.

Effect of GPER, PPARα, and PPARγ blockage on cholesterol content and progesterone secretion by mouse Leydig cells

Independent of the antagonist used, cholesterol content in Leydig cells was decreased (P < 0.05) when compared to controls (*Fig. 10A*). Treatment with the GPER antagonist resulted in abated (P < 0.001) Leydig cell progesterone secretion in comparison to controls (*Fig. 10B*). Decreased (P < 0.05, P < 0.01) progesterone secretion was seen in cells treated with all antagonists when used in combinations. Treatment with the PPARα antagonist alone resulted in decreased (P < 0.05) progesterone secretion, while treatment with the PPARγ antagonist markedly increased (P < 0.001) hormone levels.

DISCUSSION

In recent years, proteins that play a role in lipid metabolism have been newly identified. The functional characterization, including clinical application, have been presented (37, 38). As discoveries are made concerning GPER control of testicular cells, as well as PPAR-dependent regulation in various tissues, our insight into the molecular mechanisms of GPER-PPAR interaction on lipid homeostasis has shown to be significant in Leydig cell physiology. In previous studies, we reported altered Leydig cell number and volume resulted in perturbation in sex steroid secretion and signaling in mouse testis after GPER blockage (39). Herein, age-dependent effects on steroidogenic protein expression, together with LH and cholesterol concentration changes, were revealed in mice with pharmacologically blocked GPER. To our knowledge, the effects on pituitary gonadotropin levels, as well as cholesterol storage and processing, through changes in expression of acting at first step of Leydig cell steroidogenesis; LHR, StAR and TSPO in mice are reported for the first time.

Although steroidogenesis is affected, transgenic studies in knockout GPER mice demonstrate undisturbed spermatogenesis (40). In human and rat testes, GPER was the main receptor driving downregulation of steroidogenic function under excess estradiol conditions (41). The critical role of GPER was highlighted in zebrafish oocyte maturation and steroidogenesis (42). In seasonal breeders such as bank voles, GPER levels are regulated by estrogens without photoperiod influence which is not the case for canonical estrogen receptors (19). Thus, GPER is emerging as an important regulatory component of Leydig cell biology.

GPER blockage affected its interactions with PPARα and PPARγ in Leydig cells during various periods of the mouse life span. This was also observed in MA-10 cells, *via* GPER and PPARγ expression modulations, confirming this Leydig cell line has biochemical properties closest to Leydig cells of mature testis. PPARα showed diverse properties and/or regulation between *in vivo* and *in vitro* conditions. Notably, multiple factors, that create testicular milieu *in vivo* (*e.g.* hormones) and may potentially influence PPARα expression, are absent in *in vitro* system. Differences in *in vivo* and *in vitro* experimental design should be also taken into attention.

PPARs up-regulate expression of enzymes acting for the conversion of fatty acid esters (43). Upon activation of target molecules, PPAR forms a heterodimer with the retinoid X receptor, which then binds to the peroxisome proliferator response element (PPRE) and modulates gene transcription (44). In Leydig cells, PPAR-dependent molecules and their regulation is not well known: however, it seems that such regulation involves several factors also those not directly implicated in lipid homeostasis. Kowalewski *et al.*, (45) demonstrated that PPARγ increases Leydig cell sensitivity to cAMP stimulation which is linked to increased activity of steroid molecules. In females, the control of PPAR upon gonadal steroidogenic function starts at the hypothalamus-pituitary level (46). Herein, we showed diverse regulation of steroidogenesis controlling molecules in Leydig cells by GPER-

PPAR interplay dependent on protein biochemical nature, function, place of action. Steroidogenic cells have been shown to produce a maximum amount of steroid in the absence of hormonal stimulation but within a specifically defined microenvironment *e.g.* with cholesterol-like substrates (47). Data by Eacker *et al.*, (48) confirms LH stimulation of transcription of genes involved in steroidogenesis and those required for cholesterol synthesis and uptake. On the other hand, a subset of cholesterol biosynthetic genes can be down-regulated by produced sex steroids, providing additional feedback regulation in Leydig cells. Various targets of LH signaling can be affected by hypothalamus-pituitary axis disruption too. In the present study, either blockage of PPARα or PPARγ alone, or together with GPER, modulated the cholesterol status and steroid secretion in Leydig cells directly and/or indirectly through steroidogenesis-controlling molecules. In porcine ovarian steroidogenic cells local regulators including gonadotropins and steroid hormones modulated PPAR expression (49). Differences in progesterone level can be a result of modulation of different steps of cholesterol synthesis, storage and processing in Leydig cells treated with antagonists. In rats, high amounts of cholesterol in diet severely disrupted intratesticular estradiol secretion and action (50).

In the literature only scarce data exists on steroidogenic proteins interactions and control including GPER and PPAR alone. Matsuo and Strauss (51) demonstrated that PPARs strongly affect P450scc in choriocarcinoma cells (JEG-3). Depending upon cholesterol availability, steroid production was diversely modified without changes in P450scc activity. However, P450scc, StAR, and/or other steroidogenesis-regulating molecules play a critical role in the mechanism by which Leydig cell steroidogenesis is reduced following treatment with chemical and physical factors, ultimately leading to perturbations in normal physiology and/or precocious and natural ageing (52, 53). Additionally, Borch *et al.*, (54) reported a concomitant reduction of P450scc, StAR, and PPARγ protein levels in rat fetal Leydig cells after diethylhexyl phthalate exposure, indicating a functional link between these steroidogenesis-regulating molecules and pathological processes. Moreover, diisobutyl phthalate and other PPAR agonists induced changes in PPARα and other steroidogenesis-contorting molecules in fetal rat gonads (55). In Leydig cells of aged rats, despite reduced amounts of TSPO, its direct activation is able to increase testosterone production (56). At this juncture, we do not know which molecule and/or reaction of the steroidogenic pathway is rate-limiting in mouse Leydig cells. Also, it is unknown if mechanistic changes occur in any reactions under receptor blockage- and/or age-dependent conditions.

Activation of PPARα, with the involvement of StAR-TSPO *in utero*, decreased reproductive function in rodent males (57). Recently, lipid droplet regulation by PPARs and perilipin in various tissues (in liver by PPARα, in adipose tissue and skeletal muscle by PPARγ) was presented (58). In transcriptional control of human and rat hepatic lipid metabolism, HMGCR regulation through PPARα and PPARγ is essential (59, 60). In addition, HMGCR regulation of binding PPARα inhibitors and, in turn, control of brain function, including brain steroidogenesis in mice was demonstrated (61).

Recently, other regulatory mechanisms affecting enzymes beyond HMGCR were introduced (62). These mechanisms, may lay upon HMGCR induction of anchorage-independent growth in breast epithelial cells, cell transformation, and invasive properties (63). The present data shows a link between increased lipid metabolism (*via* P450scc and HMGCR activity) and increased migration characteristics of Leydig cells. Indeed, inhibition of HMGCR activity, perturbs germ cell survival and cell migration that lead to tumor testis transformation in mice (64).

In contrast to PLIN, P450scc and HMGCR, HSL was down-regulated by GPER and PPARs antagonists, that reflects role of GPER and PPARs in the control of HSL and lipid metabolism, as shown previously in hepatocytes and nervous system (65, 66).

It is possible that extracellular signals are obtained by GPER while endogenous signals are recognized by PPAR. Both receptors could then interact with each other, modulating Leydig cell steroidogenic function, both directly and indirectly, through supervision of cell morphological structure and behavior (*e.g.* proliferation, growth, and migration). In Leydig cells, GPER and PPAR can functioning as an integrated two-receptor, PPAR-GPR40 (Gq-coupled free fatty acid receptor), signal transduction pathway, as in human endothelial cells. (67).

Directed cell migration requires coordinated activation of several processes: cell polarization and elongation, formation of finger-like protrusions, attachment to components of the extracellular matrix, and contraction of the cell body to generate a force for the movement (68). Cell migration is induced in response to pro-migratory factors, including growth factors and chemokines but also by signaling lipids such as diacyloglycerol, lipoprotein lipase, and prostaglandins (69). Our data shows that in response to the GPER-PPAR interaction, modification of lipid metabolism-regulating molecules acting in couples (LHR and PKA, StAR and TSPO, PLIN, P450scc and HMGCR) can effect cell migration *via* various mechanisms: modulation of cell steroidogenic status, cytoskeletal reorganization, and/or signaling cascade activity changes that are also characteristic for tumor cells (70).

Intracellular cholesterol content affects cellular mechanical properties through the underlying cytoskeleton (71). The processes of pseudopodia extension are mediated by a diverse set of signals and different receptors (*e.g.* protease-activated receptor 2). It seems possible that, in Leydig cells, GPER, PPARα, and PPARγ can regulate cell migration, either individually or acting together. Activation of GPER suppressed migration and angiogenesis of breast cancer cells occurs through inhibition of NF-κB/IL-6 signals (72). Husueh *et al.*, (73) reported that PPARγ, and its ligands effected both proliferation and migration of vascular smooth muscle cells. The antimigratory effects of PPAR-activators has been found in endothelial cells as related to vasculature protection from pathological alterations associated with metabolic disorders (74). Recently, several studies revealed molecules linking migratory signals to the actin cytoskeleton are upregulated in invasive and metastatic cancer cells (75). That is in accord with our results additionally showing that GPER-PPAR interactions are involved in tumor biology of Leydig cell. Interestingly, one of the molecular mechanism of pseudopodia growth physiology is based on the equilibrium of phosphorylation/dephosphorylation (76). The cytoskeleton contributes to cell morphology, motility, division, and transport. Tubulin has intrinsic GTPase activity and is a promoter of receptor-independent activation of G-proteins, which is related to microfilament stability (77). Thus, these processes may exists and can be a result of increased tubulin expression in Leydig cells with PPARα and PPARγ blockage. Several studies indicate that PPARγ inhibitors reduce tumor cell growth through rapid dissolution of the microtubule network (78). In the light of the above, we propose that cytoskeleton reorganization in GPER-PPAR blocked cells can also be a primary cause of steroidogenesis modification and behavioral changes of Leydig cells.

It was reported that PPARγ activity is decreased because of overactivation of the WNT/β-catenin signaling, thereby effecting cellular thermodynamics (79). Activation of GPER induces coronary artery relaxation by concurrent inhibition of RhoA/Rho kinase by Epac/Rap1 and PKA (80). Herein, during

GPER-PPARα blockage PI3K/Akt pathway was activated while GPER-PPARγ induced Raf/Ras downstream, leading to cell steroidogenic function modulation and *via* its migration competencies, cytoskeleton structure, and phosphatases activity. It is worth to mentioning that each of the studied receptors exerted an individual effect on one of the enzyme from signaling cascades: GPER on Ras; PPARα on Raf; and PPARγ on Akt, indicating a dependency of that enzyme to specific receptor regulation. This can be a new direction for studies examining the role of other protein coupled interactions in Leydig cell physiology. Akt is known to regulate endothelial cell migration through its activation by various PPAR activators (75). Raf-1 is a main effector of Ras GTPase, and its regulator is protein phosphatase 5 (PP5) (81). PP5 is responsible for mediation of lipid metabolism through PPARγ in mouse embryonic fibroblast cells (82). By PP5-mediated dephosphorylation of Ser 338, Raf-1 activity is inhibited. Of note, tyrosine phosphatase (SHP2) is a crucial StAR regulator (2). Noteworthy, the MAP kinase phosphatase family has a role in downregulation of the hormonal signal in ERK-dependent processes such as steroid synthphlppesis and proliferation. The ERK-pathway is activated by PPARγ in proadipocyte differentiation (83), while in tumor prostate cells, PPARγ acts through the MEK-pathway maintaining their pathological features as well as other cellular processes in various cell lineages (84, 85). Phosphatase PHLPP, through dephosphorylation of Akt, promoted apoptosis and suppressed tumor growth in several tumor cell lines (86). In the present study, Leydig cells, phosphatases activity status corresponded with downregulation of signaling molecules such as Raf, Ras, and PI3K, but not Akt, in response to particular antagonists. It was demonstrated that PI3K/AKT/PTEN phosphatases play a pivotal role in neuroprotection, enhancing cell survival by stimulating cell proliferation, and inhibiting apoptosis where PTEN is negatively regulated through lipid phosphatase activity (87). Ovarian follicle nutrient flux includes the PI3K/Akt with PPAR action on steroidogenesis (88). The after mentioned data clearly indicates that numerous signaling cascades and molecules take part in complex and multilevel regulation of the GPER-PPAR of cell lipid homeostasis together with control through it cell morphology and behavior however they linkage needs further detailed elucidation.

Our data shows that GPER inactivation affects the morpho-functional status of both mature and aged Leydig cells. This receptor is an important partner of PPARα and PPARγ in regulating the steroidogenic status of Leydig cells through direct and/or indirect control at diverse regulatory levels (i) steroidogenesis-controlling molecules including central endocrine axis, (ii) cytoskeleton structure together with migratory competences, (iii) phosphates activity, and (iv) signal transmitting molecule activity. In the above processes, the action of GPER and PPARα, through PI3K/Akt pathway, is involved, while PPARγ acts trough Ras/Raf pathway. In addition, each receptor specifically controls individual molecules of these pathways.

This study provides insight into the possible new regulatory couple GPER-PPAR. Therefore, for future studies we propose the importance of GPER-PPAR 'neopartnership' in regulating Leydig cell morphology and steroid biosynthesis throughout male physiological development and pathology, with special attention paid to tumorigenesis.

Author contributions: Authors' contribution to the work described in the paper: E. Gorowska-Wojtowicz, P. Dutka, M. Kudrycka, P. Pawlicki, A. Milon, B.J. Plachno, W. Tworzydlo, L. Pardyak, A. Kaminska, A. Hejmej, M. Kotula-Balak. performed research. A. Hejmej, B. Bilinska, M. Kotula-Balak analyzed the data. M. Kotula-Balak designed the research study and wrote the paper. All authors have read and approved the final version of the manuscript.

Acknowledgements: This work was supported by a grant OPUS12 2016/23/B/NZ4/01788 from National Science Centre, Poland.

Conflict of interests: None declared.

REFERENCES

1. Miller WL. Steroid hormone synthesis in mitochondria. *Mol Cell Endocrinol* 2013; 379: 62-73.
2. Paz C, Cornejo Maciel F, Gorostizaga A, *et al.* Role of protein phosphorylation and tyrosine phosphatases in the adrenal regulation of steroid synthesis and mitochondrial function. *Front Endocrinol* (*Lausanne*) 2016; 7: 60. doi: 10.3389/fendo.2016.00060
3. Sewer MB, Li D. Regulation of steroid hormone biosynthesis by the cytoskeleton. *Lipids* 2008; 43: 1109-1115.
4. Schmidt A, Endo N, Rutledge SJ, Vogel R, Shinar D, Rodan GA. Identification of a new member of the steroid hormone receptor superfamily that is activated by a peroxisome proliferator and fatty acids. *Mol Endocrinol* 1992; 6: 1634-1641.
5. Aoyama T, Peters JM, Iritani N, *et al.* Altered constitutive expression of fatty acid-metabolizing enzymes in mice lacking the peroxisome proliferator-activated receptor alpha (PPARalpha). *J Biol Chem* 1998; 273: 5678-5684.
6. Watanabe K, Fujii H, Takahashi T, *et al.* Constitutive regulation of cardiac fatty acid metabolism through peroxisome proliferator-activatedreceptor alpha associated with age-dependent cardiac toxicity.
7. Kamijo Y, Hora K, Tanaka N, *et al.* Identification of functions of peroxisome proliferator-activated receptor alpha in proximal tubules. *J Am Soc Nephrol* 2002; 13: 1691-1702.
8. Braissant O, Foufelle F, Scotto C, Dauca M, Wahli W. Differential expression of peroxisome proliferator-activated receptors (PPARs): tissue distribution of PPAR-alpha, -beta, and -gamma in the adult rat. *Endocrinology* 1996; 137: 354-366.
9. Harada Y, Tanaka N, Ichikawa M, *et al.* PPARα-dependent cholesterol/testosterone disruption in Leydig cells mediates 2,4-dichlorophenoxyacetic acid-induced testicular toxicity in mice. *Arch Toxicol* 2016; 90: 3061-3071.
10. Biegel LB, Hurtt ME, Frame SR, O'Connor JC, Cook JC. Mechanisms of extrahepatic tumor induction by peroxisome proliferators in male CD rats. *Toxicol Sci* 2001; 1: 44-55.
11. Kostadinova R, Wahli W, Michalik L. PPARs in diseases: control mechanisms of inflammation. *Cur Med Chem* 2005; 12: 2995-3009.
12. Lehrke M, Lazar MA. The many faces of PPARγ. *Cell* 2005; 123: 993-999.
13. Jahrling JB, Hernandez CM, Denner L, Dineley KT. PPARγ recruitment to active ERK during memory consolidation is required for Alzheimer's disease-related cognitive enhancement. *J Neurosci* 2014; 34: 4054-4063.
14. Burgermeister E, Seger R. PPARγ and MEK interactions in cancer. *PPAR Res* 2008; 2008; 309469. doi: 10.1155/2008/309469
15. Lucas TF, Pimenta MT, Pisolato R, Lazari MF, Porto CS. 17beta-estradiol signaling and regulation of Sertoli cell function. *Spermatogenesis* 2011; 1: 318-324.
16. Chimento A, Sirianni R, Casaburi I, Pezzi V. GPER signaling in spermatogenesis and testicular tumors. *Front Endocrinol* (*Lausanne*) 2014; 5: 30. doi: 10.3389/fendo.2014.00030

17. Rago V, Giordano F, Brunelli E, Zito D, Aquila S, Carpino A. Identification of G protein-coupled estrogen receptor in human and pig spermatozoa. *J Anat* 2014; 224: 732-736.
18. Sandner F, Welter H, Schwarzer JU, Kohn FM, Urbanski HF, Mayerhofer A. Expression of the oestrogen receptor GPER by testicular peritubular cells is linked to sexual maturation and male fertility. *Andrology* 2014; 2: 695-701.
19. Zarzycka M, Gorowska-Wojtowicz E, Tworzydlo W, *et al.* Are aryl hydrocarbon receptor and G-protein-coupled receptor 30 involved in the regulation of seasonal testis activity in photosensitive rodent-the bank vole (Myodes glareolus)? *Theriogenology* 2016; 86: 674-686.
20. Scaling AL, Prossnitz ER, Hathaway HJ. GPER mediates estrogen-induced signaling and proliferation in human breast epithelial cells and normal and malignant breast. *Horm Cancer* 2014; 5:146-160.
21. Liu C, Liao Y, Fan S, *et al.* G protein-coupled estrogen receptor (GPER) mediates NSCLC progression induced by 17β-estradiol (E2) and selective agonist G1. *Med Oncol* 2015; 32: 104. doi: 10.1007/s12032-015-0558-2
22. Barton M, Prossnitz ER. Emerging roles of GPER in diabetes and atherosclerosis. *Trends Endocrinol Metab* 2015; 26: 185-192.
23. Dennis MK, Burai R, Ramesh C, *et al.* In vivo effects of a GPR30 antagonist. *Nat Chem Biol* 2009; 5: 421-427.
24. Kang WB, Cong Y, Ru JY, *et al.* Osteoprotective effect of combination therapy of low-dose oestradiol with G15, a specific antagonist of GPR30/GPER in ovariectomy-induced osteoporotic rats. *Biosci Rep* 2015; 35: e00239. doi: 10.1042/BSR20150146
25. Ascoli M. Characterization of several clonal lines of cultured Leydig tumor cells: gonadotropin receptors and steroidogenic responses. *Endocrinology* 1981; 108: 88-95.
26. M. Ascoli M, Puett D. Gonadotropin binding and stimulation of steroidogenesis in Leydig tumor cells. *Proc Natl Acad Sci USA* 1978; 75: 99-102.
27. Lee G, Elwood F, McNally J, *et al.* T0070907, a selective ligand for peroxisome proliferator-activated receptor gamma, functions as an antagonist of biochemical and cellular activities. *J Biol Chem* 2002; 277: 19649-19657.
28. Schaefer KL, Wada K, Takahashi H, *et al.* Peroxisome proliferator-activated receptor gamma inhibition prevents adhesion to the extracellular matrix and induces anoikis in hepatocellular carcinoma cells. *Cancer Res* 2005; 65: 2251-2259.
29. Dennis MK, Field AS, Burai R, *et al.* Identification of a GPER/GPR30 antagonist with improved estrogen receptor counterselectivity. *J Steroid Biochem Mol Biol* 2011; 127: 358-366.
30. An Z, Muthusami S, Yu JR, Park WY. T0070907, a PPARγ inhibitor, induced G2/M arrest enhances the effect of radiation in human cervical cancer cells through mitotic catastrophe. *Reprod Sci* 2014; 21: 1352-1361.
31. Kurzynska A, Bogacki M, Chojnowska K, Bogacka I. Peroxisome proliferator activated receptor ligands affect progesterone and 17β-estradiol secretion by porcine corpus luteum during early pregnancy. *J Physiol Pharmacol* 2014; 65: 709-717.
32. Carnesecchi J, Malbouyres M, de Mets R, *et al.* Estrogens induce rapid cytoskeleton re-organization in human dermal fibroblasts via the non-classical receptor GPR30. *PLoS One* 2015; 10: e0120672. doi: 10.1371/journal.pone.0120672
33. Treen AK, Luo V, Chalmers JA, *et al.* Divergent regulation of ER and Kiss genes by 17β-estradiol in hypothalamic ARC versus AVPV models. *Mol Endocrinol* 2016; 30: 217-233.
34. Smolen AJ. Image analytic techniques for quantification of immunocytochemical staining in the nervous system. In: Quantitative and Qualitative Microscopy, Conn PM. (ed.), San Diego, Academic Press 1999, pp. 208-229.
35. Kotula-Balak M, Chojnacka K, Hejmej A, Galas J, Satola M, Bilinska B. Does 4-tert-octylphenol affect estrogen signaling pathways in bank vole Leydig cells and tumor mouse Leydig cells in vitro? *Reprod Toxicol* 2013; 39: 6-16.
36. Pawlicki P, Milon A, Zarzycka M, *et al.* Does signaling of estrogen-related receptors affect structure and function of bank vole Leydig cells? *J Physiol Pharmacol* 2017; 68: 459-476.
37. Veenman L, Gavish M. The role of 18 kDa mitochondrial translocator protein (TSPO) in programmed cell death, and effects of steroids on TSPO expression. *Cur Mol Med* 2012; 12: 398-412.
38. Oresti GM, Garcia-Lopez J, Aveldano MI, Del Mazo J. Cell-type-specific regulation of genes involved in testicular lipid metabolism: fatty acid-binding proteins, diacylglycerol acyltransferases, and perilipin 2. *Reproduction* 2013; 146: 471-480.
39. Kotula-Balak M, Pawlicki P, Milon A, *et al.* The role of G-protein coupled membrane estrogen receptor in mouse Leydig cell function - in vivo and in vitro evaluation. *Tissue Cell Res* 2018; June 6. doi: 10.1007/s00441-018-2861-7
40. Prossnitz ER, Hathaway HJ. What have we learned about GPER function in physiology and disease from knockout mice? *J Steroid Biochem Mol Biol* 2015; 153: 114-126.
41. Vaucher L, Funaro MG, Mehta A, *et al.* Activation of GPER-1 estradiol receptor downregulates production of testosterone in isolated rat Leydig cells and adult human testis. *PLoS One* 2014; 9: e92425. doi: 10.1371/journal.pone.0092425
42. Pang Y, Thomas P. Role of G protein-coupled estrogen receptor 1, GPER, in inhibition of oocyte maturation by endogenous estrogens in zebrafish. *Dev Biol* 2010; 342: 194-206.
43. Tyagi S, Gupta P, Saini AS, Kaushal C, Sharma S. The peroxisome proliferator-activated receptor: a family of nuclear receptors role in various diseases. *J Adv Pharm Technol Res* 2011; 2: 236-240.
44. Pawlak M, Lefebvre P, Staels B. Molecular mechanism of PPARα action and its impact on lipid metabolism, inflammation and fibrosis in non-alcoholic fatty liver disease. *J Hepatol* 2015; 62: 720-733.
45. Kowalewski MP, Dyson MT, Manna PR, Stocco DM. Involvement of peroxisome proliferator-activated receptor gamma in gonadal steroidogenesis and steroidogenic acute regulatory protein expression. *Reprod Fertil Dev* 2009; 21: 909-922.
46. Shiue YL, Chen LR, Tsai CJ, Yeh CY, Huang CT. Emerging roles of peroxisome proliferator-activated receptors in the pituitary gland in female reproduction. *Biomarkers Genomic Med* 2013; 22: 553-561.
47. Chaudhary LR, Stocco DM. Stimulation of cholesterol side-chain cleavage enzyme activity by cAMP and hCG in MA-10 Leydig tumor cells. *Biochimie* 1988; 70: 1799-1806.
48. Eacker SM, Agrawal N, Qian K, Dichek HL, Gong EY, Lee K, Braun RE. Hormonal regulation of testicular steroid and cholesterol homeostasis. *Mol Endocrinol* 2008; 22: 623-635.
49. Kurowska P, Chmielinska J, Ptak A, Rak A. Expression of peroxisome proliferator-activated receptors is regulated by gonadotropins and steroid hormones in in vitro porcine ovarian follicles. *J Physiol Pharmacol* 2017; 68: 823-832.
50. Gregoraszczuk E, Slupecka M, Wolinski J, *et al.* Maternal high-fat diet during pregnancy and lactation had gender difference effect on adiponectin in rat offspring. *J Physiol Pharmacol* 2016; 67: 543-553.
51. Matsuo H, Strauss JF. Peroxisome proliferators and retinoids affect JEG-3 choriocarcinoma cell function. *Endocrinology* 1994; 135: 1135-1145.

52. Luo L, Chen H, Zirkin BR. Are Leydig cell steroidogenic enzymes differentially regulated with aging? *J Androl* 1996; 17: 509-515.
53. Diamanti-Kandarakis E, Bourguignon JP, Giudice LC, *et al.* Endocrine-disrupting chemicals: an endocrine society scientific statement. *Endocrine Rev* 2009; 30: 293-342.
54. Borch J, Metzdorff SB, Vinggaard AM, Brokken L, Dalgaard M. Mechanisms underlying the anti-androgenic effects of diethylhexyl phthalate in fetal rat testis. *Toxicology* 2006; 223: 144-155.
55. Boberg J, Metzdorff S, Wortziger R, *et al.* Impact of diisobutyl phthalate and other PPAR agonists on steroidogenesis and plasma insulin and leptin levels in fetal rats. *Toxicology* 2008; 250: 75-81.
56. Chung JY, Chen H, Midzak A, Burnett AL, Papadopoulos V, Zirkin B. Drug ligand-induced activation of translocator protein (TSPO) stimulates steroid production by aged brown Norway rat Leydig cells. *Endocrinology* 2013; 154: 2156-2165.
57. Nepelska M. Peroxisome proliferator-activated receptors (PPARs) activation leading to reproductive toxicity in rodents. Adverse Outcome Pathways: From Research to Regulation. European Union Reference Laboratory. Alternatives for Animal Testing. www.jrc.ec.europa.eu 2014
58. de la Rosa Rodriguez MA, Kersten S. Regulation of lipid droplet-associated proteins by peroxisome proliferator-activated receptors. *Biochim Biophys Acta* 2017; 1862: 1212-1220.
59. Arimura N, Horiba T, Imagawa M, Shimizu M, Sat R. The peroxisome proliferator-activated receptor gamma regulates expression of the perilipin gene in adipocytes. *J Biol Chem* 2004; 279: 10070-10076.
60. Goldwasser J, Cohen PY, Yang E, Balaguer P, Yarmush ML, Nahmias Y. Transcriptional regulation of human and rat hepatic lipid metabolism by the grapefruit flavonoid naringenin: role of PPARalpha, PPARgamma and LXRalpha. *PLoS One* 2010; 5: e12399. doi: 10.1371/journal.pone.0012399
61. Roy A, Jana M, Kundu M, *et al.* HMG-CoA reductase inhibitors bind to PPARα to upregulate neurotrophin expression in the brain and improve memory in mice. *Cell Metab* 2015; 22: 253-265.
62. Sharpe LJ, Brown, AJ. Controlling cholesterol synthesis beyond 3-hydroxy-3-methylglutaryl-CoA reductase (HMGCR). *J Biol Chem* 2013; 288: 18707-18715.
63. Clendening JW, Pandyra A, Boutros PC, *et al.* Dysregulation of the mevalonate pathway promotes transformation. *Proc Nat Acad Sci USA* 2010; 107: 15051-15056.
64. Ding J, Jiang D, Kurczy M, *et al.* Inhibition of HMG CoA reductase reveals an unexpected role for cholesterol during PGC migration in the mouse. *BMC Dev Biol* 2008; 31: 120. doi: 10.1186/1471-213X-8-120
65. Deng T, Shan S, Li PP, *et al.* Peroxisome proliferator-activated receptor-gamma transcriptionally up-regulates hormone-sensitive lipase via the involvement of specificity protein-1. *Endocrinology* 2006; 147: 875-884.
66. Lopez M, Tena-Sempere M. Estradiol effects on hypothalamic AMPK and BAT thermogenesis: a gateway for obesity treatment? *Pharmacol Ther* 2017; 178: 109-122.
67. Wang S, Awad KS, Elinoff JM, *et al.* G protein-coupled Receptor 40 (GPR40) and peroxisome proliferator-activated peceptor γ (PPARγ): an integrated two-receptor signaling pathway. *J Biol Chem* 2015; 290: 19544-19557.
68. Friedl P, Wolf K. Proteolytic and non-proteolytic migration of tumour cells and leucocytes. *Biochem Soc Symp* 2003; 70: 277-285.
69. Ge L, Ly Y, Hollenberg M, DeFea K. A beta-arrestin-dependent scaffold is associated with prolonged MAPK activation in pseudopodia during protease-activated receptor-2-induced chemotaxis. *J Biol Chem* 2003; 278: 34418-34426.
70. Hanahan D, Coussens LM. Accessories to the crime: functions of cells recruited to the tumor microenvironment. *Cancer Cell* 2012; 21: 309-322.
71. Sun M, Northup N, Marga F, *et al.* The effect of cellular cholesterol on membrane-cytoskeleton adhesion. *J Cell Sci* 2007; 120: 2223-2231.
72. Liang S, Chen Z, Jiang G, *et al.* Activation of GPER suppresses migration and angiogenesis of triple negative breast cancer via inhibition of NF-κB/IL-6 signals. *Cancer Lett* 2017; 386: 12-23.
73. Hsueh WA, Jackson S, Law RE. Control of vascular cell proliferation and migration by PPAR-gamma: a new approach to the macrovascular complications of diabetes. *Diabetes Care* 2001; 24: 392-397.
74. Goetze S, Eilers F, Bungenstock A, *et al.* PPAR activators inhibit endothelial cell migration by targeting Akt. *Bioch Biophys Res Comm* 2002; 293: 1431-1437.
75. Yamaguchi H, Condeelis J. Regulation of the actin cytoskeleton in cancer cell migration and invasion. *Bioch Biophys Acta* 2007; 1773: 642-652.
76. Ura S, Pollitt AY, Veltman DM, Morrice NA, Machesky LM, Insall RH. Pseudopod growth and evolution during cell movement is controlled through SCAR/WAVE dephosphorylation. *Curr Biol* 2012; 22: 553-561.
77. Schappi JM, Krbanjevic A, Rasenick MM. Tubulin, actin and heterotrimeric G proteins: coordination of signaling and structure. *Bioch Biophys Acta* 2014; 1838: 674-681.
78. Schaefer KL. PPARγ inhibitors as novel tubulin-targeting agents. *PPAR Res* 2008; 2008: 785405. doi: 10.1155/2008/785405
79. Lecarpentier Y, Claes V, Vallee A, Hebert JL. Thermodynamics in cancers: opposing interactions between PPAR gamma and the canonical WNT/beta-catenin pathway. *Clin Transl Med* 2017; 6: 14. doi: 10.1186/s40169-017-0144-7
80. Yu X, Zhang Q, Zhao Y, *et al.* Activation of G protein-coupled estrogen receptor 1 induces coronary artery relaxation via Epac/Rap1-mediated inhibition of RhoA/Rho kinase pathway in parallel with PKA. *PLoS One* 2017; 2: e0173085. doi: 10.1371/journal.pone.0173085
81. von Kriegsheim A, Pitt A, Grindlay GJ, Kolch W, Dhillon AS. Regulation of the Raf-MEK-ERK pathway by protein phosphatase 5. *Nat Cell Biol* 2006; 8: 1011-1016.
82. Hinds TD, Stechschulte LA, Cash HA, *et al.* Protein phosphatase 5 mediates lipid metabolism through reciprocal control of glucocorticoid receptor and peroxisome proliferator-activated receptor-γ (PPARγ). *J Biol Chem* 2011; 286: 42911-42922.
83. Kim J, Han DC, Kim JM, *et al.* PPAR gamma partial agonist, KR-62776, inhibits adipocyte differentiation via activation of ERK. *Cell Mol Life Sci* 2009; 66:1766-1781.
84. Bolden A, Bernard L, Jones D, Akinyeke T, Stewart LV. The PPARgamma agonist troglitazone regulates Erk 1/2 phosphorylation via a PPARγ-independent, MEK-dependent pathway in human prostate cancer cells. *PPAR Res* 2012; 2012: 929052. doi: 10.1155/2012/929052
85. McCubrey JA, Steelman LS, Chappell WH, *et al.* Roles of the Raf/MEK/ERK pathway in cell growth, malignant transformation and drug resistance. *Biochim Biophys Acta* 2007; 1773: 1263-1284.
86. Gao T, Furnari F, Newton AC. PHLPP: a phosphatase that directly dephosphorylates Akt, promotes apoptosis, and suppresses tumor growth. *Mol Cell* 2005; 18: 13-24.

87. Kitagishi Y, Matsuda S. Diets involved in PPAR and PI3K/AKT/PTEN pathway may contribute to neuroprotection in a traumatic brain injury. *Alzheimer's Res Ther* 2013; 5: 42. doi: 10.1186/alzrt208
88. Dupont J, Reverchon M, Cloix L, Froment P, Rame C. Involvement of adipokines, AMPK, PI3K and the PPAR signaling pathways in ovarian follicle development and cancer. *Int J Dev Biol* 2012; 56: 959-967.

Received: April 27, 2018
Accepted: June 30, 2018

Author's address: Dr. Malgorzata Kotula-Balak, Department of Endocrinology, Institute of Zoology and Biomedical Research, Jagiellonian University, 9 Gronostajowa Street, 30-387 Cracow, Poland.
E-mail: malgorzata.kotula-balak@uj.edu.pl